CR 159469

FEASIBILITY STUDY FOR A SECONDARY Na/S BATTERY

FINAL REPORT
for Period October 1, 1977 – September 30, 1978

by

K. M. Abraham
R. Schiff
S. B. Brummer

EIC Corporation
55 Chapel Street
Newton, Massachusetts 02158

Prepared for
NATIONAL AERONAUTICS AND SPACE ADMINISTRATION
Cleveland, Ohio 44135

January, 1979

CONTRACT NO NAS3-21028

NASA-Lewis Research Center
Cleveland, Ohio 44135
Joseph Singer, Project Manager

FEASIBILITY STUDY FOR A SECONDARY Na/S BATTERY

FINAL REPORT

for Period October 1, 1977 - September 30, 1978

by

K. M. Abraham
R. Schiff
S. B. Brummer

EIC Corporation
55 Chapel Street
Newton, Massachusetts 02158

Prepared for

NATIONAL AERONAUTICS AND SPACE ADMINISTRATION
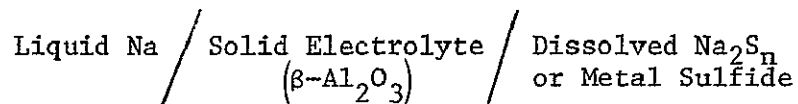Cleveland, Ohio 44135

January, 1979

CONTRACT NO. NAS3-21028

NASA-Lewis Research Center
Cleveland, Ohio 44135
Joseph Singer, Project Manager

ABSTRACT

The feasibility of a moderate temperature Na battery having the configuration

$$\text{Liquid Na} \bigg/ \begin{array}{c} \text{Solid Electrolyte} \\ \left(\beta\text{-Al}_2O_3\right) \end{array} \bigg/ \begin{array}{c} \text{Dissolved Na}_2S_n \\ \text{or Metal Sulfide} \end{array}$$

has been studied. This battery is to operate at a temperature in the range of 100-150°C. Two kinds of cathode were investigated: (i) a soluble S cathode consisting of a solution of Na_2S_n in an organic solvent and (ii) an insoluble S cathode consisting of a transition metal dichalcogenide in contact with a Na^+-ion conducting electrolyte.

Four amide solvents, dimethyl acetamide, diethyl acetamide, N-methyl acetamide and acetamide, were investigated as possible solvents for the soluble S cathode. Results of stability and electrochemical studies using these solvents are presented. The dialkyl substituted amides were found to be superior.

Although the alcohol 1,3-cyclohexanediol was found to be stable in the presence of Na_2S_n at 130°C, its Na_2S_n solutions did not appear to have suitable electrochemical properties.

The limited amount of work carried out with transition metal dichalcogenides indicates that they present interesting possibilities as cathode materials in a moderate temperature Na battery.

TABLE OF CONTENTS

LIST OF ILLUSTRATIONS

LIST OF TABLES

I. INTRODUCTION

The aim of this research program has been to investigate the feasibility of a moderate temperature, secondary Na battery utilizing S cathodes. The S cathode is either in the dissolved form as Na sulfides, Na_2S_n, $n \geq 1$, in a suitable organic or inorganic solvent, or in the insoluble form as a transition metal sulfide such as TiS_2. This system, having the cell configuration,

$$\text{Liquid Na} \; / \; \text{Solid Electrolyte} \; / \; \begin{array}{l} \text{Dissolved } Na_2S_n \\ \text{or metal sulfide} \end{array}$$
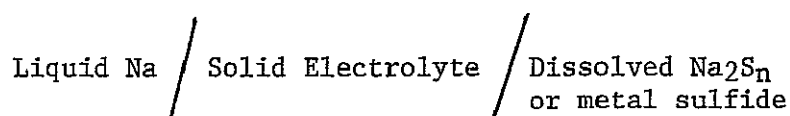
is aimed at high energy density and high power density applications and is expected to have an operating temperature in the range of 100° to 150°C. The solid electrolyte is β-Al_2O_3, an ionic conductor permeable only to Na^+ ions.

The dissolved S cathode battery would be a modification of the much researched (1,2) system,

$$\text{Liquid Na} \; / \; \beta\text{-}Al_2O_3 \; / \; \text{Molten S}$$
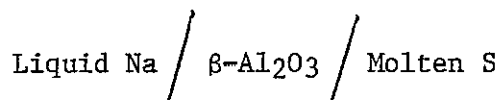
The latter system was first described by Kummer and Weber (3). In this system the fully charged cathode usually consists of a conductive graphite felt matrix imbedded in a pool of nonconductive liquid S. During discharge, Na^+ ions migrate through the solid electrolyte to form various Na polysulfides (Na_2S_n) at the surface of the porous graphite cathode. The initial discharge reaction is believed to be

$$2Na^+ + 5S + 2e^- \rightarrow Na_2S_5 \tag{1}$$
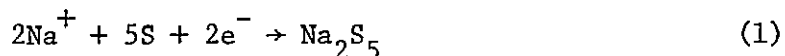
Further discharge products would involve S_4^{-2} and S_3^{-2} species, coupled with chemical steps involving ion-radical species. The operation of the system, however, is temperature-limited, and further complicated by formation of various phases, as described in its phase diagram (4). Upon discharge, insoluble Na_2S_3 precipitates out when the overall composition reaches a critical value. Because of the solidification of Na_2S_3, the lower limit of the operating temperature is 300°C. Furthermore, on charge, when the overall composition exceeds Na_2S_5, two immiscible liquid phases

1

(Na_2S_5, S) coexist; of these, the S phase is nonconductive. The porous graphite cathode operation is believed to be transport-limited (5), as a result of the high exchange current density, the complicated phase-relationship, and the nonconductivity of S-rich phase.

Since the discharge reaction stops at Na_2S_3, the attainable energy density of this system is considerably less than that corresponding to the theoretical reaction

$$2Na + S \rightarrow Na_2S \quad (\sim 700 \text{ Whr/lb}) \tag{2}$$
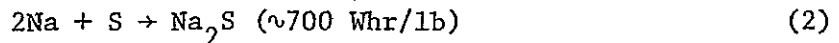
The theoretical energy density with an end-of-discharge composition of Na_2S_3 is 345 Whr/lb. The high operating temperature (>300°C) of the molten S system has introduced severe problems in the implementation of this battery concept. The successful development of the battery is contingent upon solving severe corrosion and materials problems: Cell failures occur because of accumulation of sensitive materials on the positive electrode, deterioration of the solid electrolyte or of seals, or more general corrosion (5,1). These problems fundamentally result from operation at very high temperature.

It is evident that many of the problems encountered in the Na/molten S system could be resolved by lowering the operating temperature. One way to achieve this is to use a S cathode as Na sulfides dissolved in a solvent so that the operating temperature is just above the melting point of Na, i.e., in the range of 100 to 150°C. In this case, if the solvent dissolves appreciable amounts of Na_2S, it might be possible to achieve the end-of-discharge composition closer to the theoretical Na_2S. Also the use of a solvent which dissolves appreciable amounts of Na-polysulfides (i.e., Na_2S_n where, n >> 5) could eliminate the undesirable phase separation problems encountered in the molten S battery.*

An alternative approach is to use an insoluble transition metal sulfide cathode in contact with a Na^+-ion containing electrolyte so that during discharge the cell reaction is the intercalation of Na into the sulfide lattice, as depicted in Equation 3.

$$MS_2 + Na^+ + e^- \rightleftharpoons NaMS_2 \tag{3}$$

---
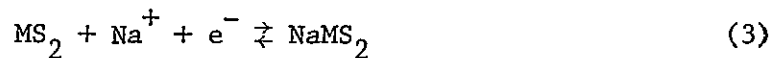
*Some solution to this problem has been found (1) by the use of metal sulfide additives such as FeS to the molten S cathode.

2

Such a battery would be analogous to the ambient temperature Li/TiS_2 cell and should operate conveniently at a temperature in the range of 100 to 150°C.

The major advantages of a moderate temperature system are:

1. Minimal problems from corrosion, seal fracture and thermal cycling.

2. Less expensive and simpler sealing procedures, e.g., the use of plastics becomes possible below 200°C.

3. Less insulation and hence less weight and cost, making smaller battery packages economical.

A preliminary battery design with a soluble S cathode indicates that for an end-of-discharge composition of Na_2S, a charged-state S solubility of 1.6M in S_8 is required to give an energy density comparable to that of a molten S battery designed for 100 Whr/lb performance. On the other hand, if the end-of-discharge product is Na_2S_2, the required S_8 concentration is $\sim$3.3M. We must, of course, take into account that compared with operation at 300-350°C, there will be some energy loss due to increased resistance of the β-Al_2O_3 and, possibly from polarization losses at the electrodes. The resistivity of β-Al_2O_3 at 300°C is $\sim$3 ohmcm and at 150°C it is 18 ohmcm. With tubes 0.8 mm thick, and discharge rates of 50 mA/cm^2, this involves a loss of 0.012V at 300°C and 0.072V at 150°C. Since the OCV is 2.08V, there is a corresponding additional loss from working at lower temperatures of 3%. In the high temperature cell, there is a further ohmic drop in the catholyte compartment about equal to that of β-Al_2O_3 (7). We can expect at least this additional loss at the lower temperature. Thus the overall energy loss from ohmic polarization in a soluble S battery would be of the order of 10%. Although the additional ohmic voltage drops associated with operation at lower temperature will effect the battery's ability to deliver the required energy density at the highest rates, it is not improbable that at less than the highest rates the soluble S battery (150°C) could achieve energy density comparable to the molten S battery (350°C). Rate goals of 25 mA/cm^2 at 1.8V seem reasonable for most applications.

The moderate temperature Na battery is analogous to the $Na/SbCl_3$ battery under development with EPRI support for electrical load-levelling (8). The latter battery is to operate at $\sim$200°C with current densities up to 25 mA/cm^2 of β-Al_2O_3. It is projected to have power densities of $\sim$50 mW/cm^2. This battery overcomes one of the major difficulties of the Na/molten S system, that of sealing. Plastic seals appear to be satisfactory (9).

3

A preliminary study, carried out at EIC (10), has shown the basic feasibility of the liquid Na/dissolved S battery concept. In this study, a liquid Na/β-Al$_2$O$_3$/dissolved S cell utilizing N,N-dimethyl acetamide (DMAC) as the S-solubilizing agent, exhibited, during short term cycling studies, good reversibility between voltage limits of 1.00 and 2.70V. The average cycling stoichiometry at 130°C corresponded to

$$5S_2^{-2} \not\rightleftarrows S_{10}^{-2} + 8e^-$$ (4)

No elemental S was formed during cell charging, but only long chain, soluble polysulfides. The major system limitation was found to be the termination of discharge (sharp voltage cut-off to 1.00V) in the vicinity of a polysulfide composition of $\sim S_2^{-2}$. The principal reasons for this appeared to be the very low solubilities of the lower order polysulfides and the consequent choking of the carbon felt current collector by the precipitated Na sulfides.

Studies (10) of Na$_2$S in various aliphatic amides had shown that its solubility decreased with increasing N-alkyl substitution. Thus acetamide (AC), N-methylacetamide (NMAC) and dimethylacetamide (DMAC) dissolved Na$_2$S in the amounts of 1.10, 0.60 and 0.0075 M/ℓ respectively at 150°C. The long term stability characteristics of these amides in the presence of Na$_2$S$_n$ had not been determined.

In the present program a detailed investigation was carried out to determine the suitability of the amides as solvents for the dissolved S cathode. The major areas of investigation were solubility determinations of Na$_2$S$_n$ in the amides at $\sim$150°C, long term stability characteristics of the amides in the presence of Na$_2$S$_n$ at 130°C, and cell cycling studies in practical configuration utilizing β-Al$_2$O$_3$ as the solid electrolyte. We have also evaluated 1,3 cyclohexanediol (CHD) as a possible solvent for the dissolved S cathode.

The transition metal disulfides, TiS$_2$ and TaS$_2$ were investigated as possible cathode candidates. The studies included determination of their long term stabilities in the presence of DMAC or DEAC at 130°C and evaluation of their cycling behavior in NaI solutions of these amides.

II. THE Na-DISSOLVED S BATTERY

The successful development of a Na-dissolved S battery is contingent upon the selection of a high boiling solvent which shows high S solubility, intrinsic thermal stability up to 150°C, and which is unreactive towards Na_2S_n. Our preliminary studies (10) had indicated that aliphatic amides were promising solvents with respect to many of these properties. Another class of solvents showing appreciable solubilities of the Na sulfides, including Na_2S, was aliphatic alcohols. The present study therefore emphasized these two class of compounds.

A.   Aliphatic Amides as Solvents for the Dissolved S Cathode

The suitability of aliphatic amides as solvents for the Na/S battery was evaluated by studying their ability to dissolve Na sulfides, Na_2S_n, (n ≥ 1) at ∿ 130°C, their long-term stability properties in the temperature range of 100-150°C, and by examining the electrochemical behavior of solutions of Na_2S_n in these amides. The aliphatic amides investigated in the program were AC, NMAC, DMAC, and diethylacetamide (DEAC). Some physical properties of these solvents are shown in Table 1.

1. Solubilities of Na_2S_n in Amide Solvents

The solubilities of Na_2S_n (n = 1, 2, 4 or 8) in each of the amides, AC, NMAC, DMAC or DEAC at 150°C were measured. The experimental procedures and the results are given below.

● General Experimental

The experiments were carried out in the absence of air and moisture using standard techniques employed for the manipulation of air sensitive compounds (11). Whenever appropriate, the handling and transfer of reagents were also carried out in an argon-filled dry box (Vacuum-Atmospheres Corporation).

● Reagents

Commercially obtained reagents were purified as described below:

Acetamide (Fisher Scientific, Lot No. 742523) was twice-recrystallized from a mixture of methanol and diethyl ether. In this procedure, acetamide was initially dissolved in anhydrous MeOH (∿1g AC/0.8 ml MeOH). It was then crystallized out by adding anhydrous diethyl ether

5

TABLE 1

SOME PHYSICAL PROPERTIES OF ACETAMIDE, N-METHYLACETAMIDE,

DIMETHYLACETAMIDE AND DIETHYLACETAMIDE

Solvent	Acetamide	N-methylacetamide	N,N-dimethyl acetamide	N,N-diethyl acetamide
M.P., °C	80.5	29.5	-20	-
B.P., °C	221.5	206.0	165	185
Density, g/ml	0.967 (120°C)	0.9503 (30°C)	0.936 (25°C)	0.924 (25°C)
Refractive Index	1.4274 (78°C)	1.4277 (30°C)	1.4351 (25°C)	-
Viscosity, CP	1.06 (120°C)	3.885 (30°C)	9.2 (25°C)	-
Dielectric Constant	74 (25°C, extrap)	186 (25°C, extrap)	27 (25°C)	-
Min. Specific Conductance ($\Omega^{-1}cm^{-1}$)	2.6×10^{-6} (94°C)	1×10^{-7} (40°C)	20 (25°C)	-

($\sim$10 ml Et$_2$O/g AC), yielding long needle-like crystals. The crystals were
further dried in vacuum ($\sim$10^{-3} torr) by continuously pumping for $\sim$20 hr.
The melting point of the twice-recrystallized material was found to be
78-79°C, very close to the reported value (12) of 80.5°C.

High purity N-methylacetamide, obtained from Aldrich Chemical Co.
(Lot No. 021777) was used after the following treatment for removal of
its water content. About 100g of NMAC was dissolved in $\sim$100 ml anhydrous
diethyl ether and the solution was then passed through a chromatography
column (1.5 cm ID and 28 cm long pyrex glass tube) packed with freshly
regenerated* Linde 4Å molecular sieves. The flow rate of the solution
through the column was maintained at $\sim$1 ml/min. The ether from the sieved
solution was removed in vacuum by collecting it in a dry ice/acetone
cooled cold trap. Final drying of the amide was carried out by continuously
pumping it in vacuum at room temperature for $\sim$20 hr. The N,N-dimethyl-
acetamide was obtained from Burdick and Jackson Laboratories, Muskegan,
Michigan. This material was of high purity, "distilled in glass" quality.
The water content of the solvent was further reduced by passing over activated
Linde 4Å molecular sieves. Diethylacetamide was vacuum distilled first
using a spinning band column (Perkin-Elmer Corp.) and then dried over
molecular sieves.

Elemental S (Ventron, random pieces), Na$_2$S (Ventron) and Na$_2$S$_4$
(Ventron) were used as-received. The polysulfides, Na$_2$S$_2$ and Na$_2$S$_8$,
were prepared from stoichiometric mixtures of Na$_2$S and Na$_2$S$_4$ respectively
with elemental S.

● Solubility Determination

The experimental setup for solubility determination is shown in
Figure 1. In a typical experiment, a mixture consisting of an excess of
the sulfide (equivalent to 2-12M S) and a known amount of the solvent (10 ml)
was taken in A and the system was thoroughly flushed with dry N$_2$. The
mixture was then heated with stirring to 150°C and maintained at this
temperature for $\sim$3 hr for equilibration. After the 3 hr of heating, any
undissolved sulfide was allowed to settle down. Thereafter, by maintaining
a N$_2$ flow, the joint at B was disconnected and an aliquot of the sample was
withdrawn for analysis of total sulfur and S^{-2}. Sampling was done by means
of a pipette which had been heated to 150°C using a heating tape. Analytical
procedures for sulfur determination are given below in detail.

---

*Fresh molecular sieves obtained from the manufacturer were regenerated by
heating at 400°C under a stream of Ar for $\sim$16 hr. About 0.30g of molecular
sieves/ml of the solution was used. Use of molecular sieves has been sug-
gested as the best method for removal of H$_2$O content of amide solvents (13).
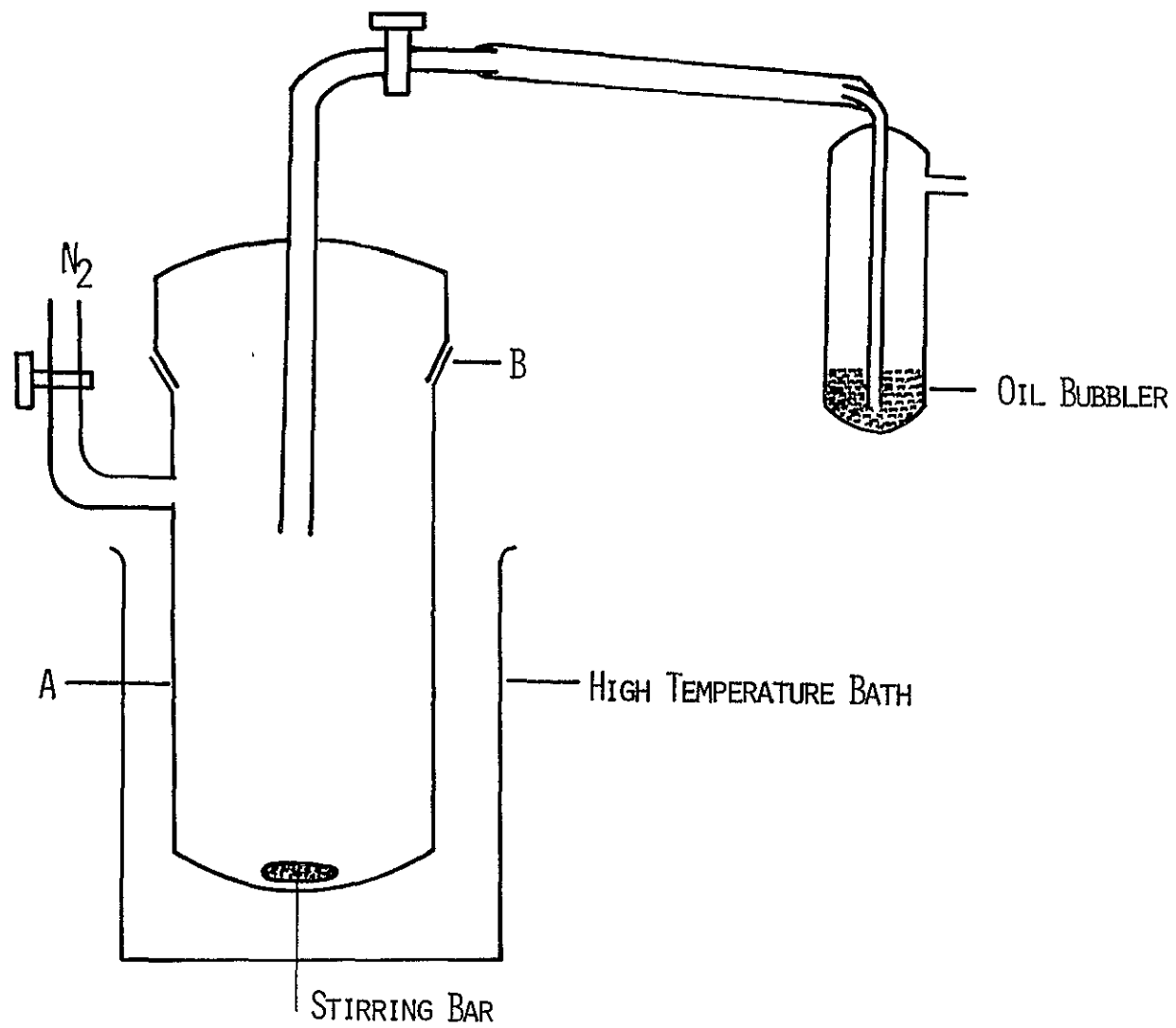
Fig. 1: Experimental set-up for determination of Na_2S_n solubilities.

● Sulfide Analysis

Sulfide analysis was carried out iodimetrically (14). It is based on the reactions,

$$I_2 + S_n^{-2} \rightarrow nS^{\circ} + 2I^- \tag{5}$$

$$2S_2O_3^{-2} + I_2 \rightarrow S_4O_6^{-2} + 2I^- \tag{6}$$
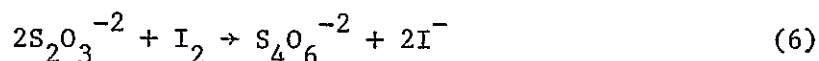
Samples of the polysulfide solution, measuring 0.50 ml, were quickly added to an excess of standardized I_2 solution (0.05N). The solution was then titrated immediately with standard thiosulfate solution (0.05N) to a starch end point. When sulfide solution is added to I_2 solution, a white to off-white precipitate is formed at the neutral point. The precipitate is elemental S, Equation 5. In the presence of excess I_2 the solution has a yellow to pink color, showing unreacted iodine. Sodium thiosulfate neutralizes this iodine according to Equation 6. The S^{-2} concentration is calculated from the amount of iodine consumed.

● Total Sulfur Analysis

Total S analysis was carried out by oxidation of the polysulfide to SO_4^{-2}, with H_2O_2 in ammoniacal medium and determination of SO_4^{-2} by titration with standardized $Ba(ClO_4)_2$ solution (15).

$$S_n^{-2} + (2n-2)\ OH^- + (2n+1)\ H_2O_2 \rightarrow nSO_4^{-2} + 4n\ H_2O \tag{7}$$
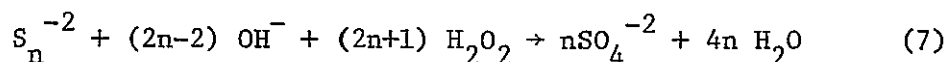
A sample of the nonaqueous polysulfide solution, 0.50 ml, was withdrawn. An excess of 50% NH_4OH, followed by excess 30% H_2O_2 were immediately added, until a colorless solution was obtained within a few minutes. The solution was then heated to boiling to destroy unreacted H_2O_2 and to insure complete oxidation of S. Heating was continued to drive off all the NH_3. The solution was then diluted to 50 ml, adjusting the pH to 2.5-4.0 with 1N HCl. (Very little or no acidification should be necessary if the NH_3 is completely removed). To a 2-5 ml aliquot, sufficient CH_3OH was added to make the solution 80%. One drop of thorin indicator solution (0.2%) was added and the solution was titrated with 0.005M standardized $Ba(ClO_4)_2$ to a pink end point.

The following procedures are important for obtaining accurate results:

For very dilute S solutions, a 1/5 dilution of the $Ba(ClO_4)_2$ should be used for titration. The end point is indicated by a change from yellow to pink. Practice is required to distinguish the intermediate orange from the final pink to within several drops (~0.02 ml/drop in a 25 ml buret). It is helpful to have, for comparison, a sample that has been titrated beyond its end point.

9

The solubilities at 150°C of Na_2S_n, $n = 1$, 2, 4 or 8, in AC, NMAC, DMAC and DEAC, respectively, are shown in Table 2. It can be seen that AC dissolves 1.06M Na_2S and NMAC dissolves 0.75M Na_2S. In general, the total S solubility in the two solvents is seen to increase with increasing polysulfide chain-length, reaching an upper limit when the S_n^{-2} chain-length is ~4. The solubility of Na_2S in AC or NMAC at 150°C is much higher than in DMAC. The observed trend of AC > NMAC > DMAC for the Na_2S-solubilizing properties of the three solvents is consistent with the increasing H-bonding ability in going from DMAC to AC. Thus from the stand point of S solubility, both AC and NMAC are superior to DMAC. However, preliminary stability studies, carried out as described previously (10) along with the solubility experiments indicated that in the long run, solutions of Na_2S_n in AC or NMAC might be less stable than solutions of Na_2S_n in DMAC or DEAC.

2. Stabilities of Amide Solvents in the Presence of Na_2S_n at 130°C

The ultimate usefulness of the amides as solvents for the S cathode in the Na/S battery is dependent upon their long term stabilities. The stability properties should include both intrinsic thermal stability and chemical compatibility with Na_2S_n at temperatures ~130°C. A thorough investigation of the long term stability characteristics of AC, NMAC, DMAC or DEAC in the presence of Na_2S_n at 130°C has been carried out. The procedure employed for this consisted of incubating amide solutions containing Na-sulfides at 130°C in sealed, evacuated glass tubes equipped with break-seals. The tubes were opened after known intervals of time (days) and the gas pressure in each tube was measured with a manometer. The solution and gas products were analyzed spectrometrically.

● Reagents

All the reagents used in these tests were carefully dried according to procedures outlined below.

N-methylacetamide, dimethylacetamide and diethylacetamide were dried and/or purified as described earlier (Section IIA.1). Acetamide was also purified by the recrystallization procedure, described in Section IIA.1. However, before recrystallization with Et_2O, the methanolic solution was dried by passing twice through a chromatography column containing molecular sieves.

Sodium monosulfide, Na_2S (Ventron), was dried by heating in vacuum at ~510°C with continuous pumping for ~16 hr. After the heating, some shrinking of the volume, coupled with a slight darkening of the sulfide, was observed.

TABLE 2

SOLUBILITY DATA FOR Na_2S_n in AMIDE SOLVENTS AT 150°C

Solvent	Na_2S (MS^{-2}/ℓ)	Na_2S_2 $(MS°/\ell)$	Na_2S_4 $(MS°/\ell)$	Na_2S_8 $(MS°/\ell)$
Acetamide	1.06	2.4	7.6	7.4
N-methylacetamide	0.75	1.8	6.2	7.0
Dimethylacetamide	0.0075	–	4.27	6.6
Diethylacetamide	†	–	3.2	6.9

_____

†Apparently none dissolved.
–Not done.

Sodium tetrasulfide, Na_2S_4 (Ventron), was also dried in vacuum at ∿215°C with continuous pumping for ∿16 hr. Elemental S (Ventron, random pieces) was also dried in vacuum at ∿110°C for ∿24 hr. At the end of the heating, all the sulfur had sublimed off and condensed onto the cooler parts of the flask in which it was heated.

● Experimental Procedure

The test vessels consisted of pyrex tubes (∿30 ml capacity) equipped with break-seals as shown in Figure 2A. Each tube was also provided with ground glass joints, A and B, for attachment to the vacuum system. The accurate volume of each tube was obtained by measuring the amount of water it required to fill the tube. In a typical experiment, weighed amounts of the sulfide or S and the amide were charged into the reaction tube inside a dry box. The tube was then evacuated at ∿10^{-3} torr and sealed off at C. The hermetically sealed tube was heated at 130°C in a constant temperature oven (Tenney Environmental Chamber) for a known period of time. Three sample tubes were used for each solution to be tested so that the tubes could be opened after different periods of heating. Before the tube was opened for measuring the gas pressure, a breaker, con-sisting of an iron rod sealed inside a glass tube was held above the break-seal on the sidearm of the sample tube using a pair of magnets wrapped in a piece of electrical tape. After attachment of the sample tube to the manometer assembly (Figure 2B) and evacuation, the break-seal was opened by dropping the breaker, and the gas pressure was measured. Since the volumes of the manometer assembly and the sample tube are known, the amount of gas (mmoles) could be calculated using the ideal gas equation,

$$PV = nRT$$

where P = pressure (atmosphere)

V = volume (liter)

T = temperature, °K

R = gas constant, 0.082 liter, atmosphere/mole/0°K

After the pressure measurements, the gases were analyzed by vapor phase IR and mass spectrometric methods. The solutions were also analyzed spectro-scopically using IR, NMR and mass spectra.

● Results and Discussion

Thermal Stabilities of Aliphatic Amides. Gas pressure measure-ments and spectroscopic data indicated that the aliphatic amides are thermally stable for at least 21 days at 130°C.
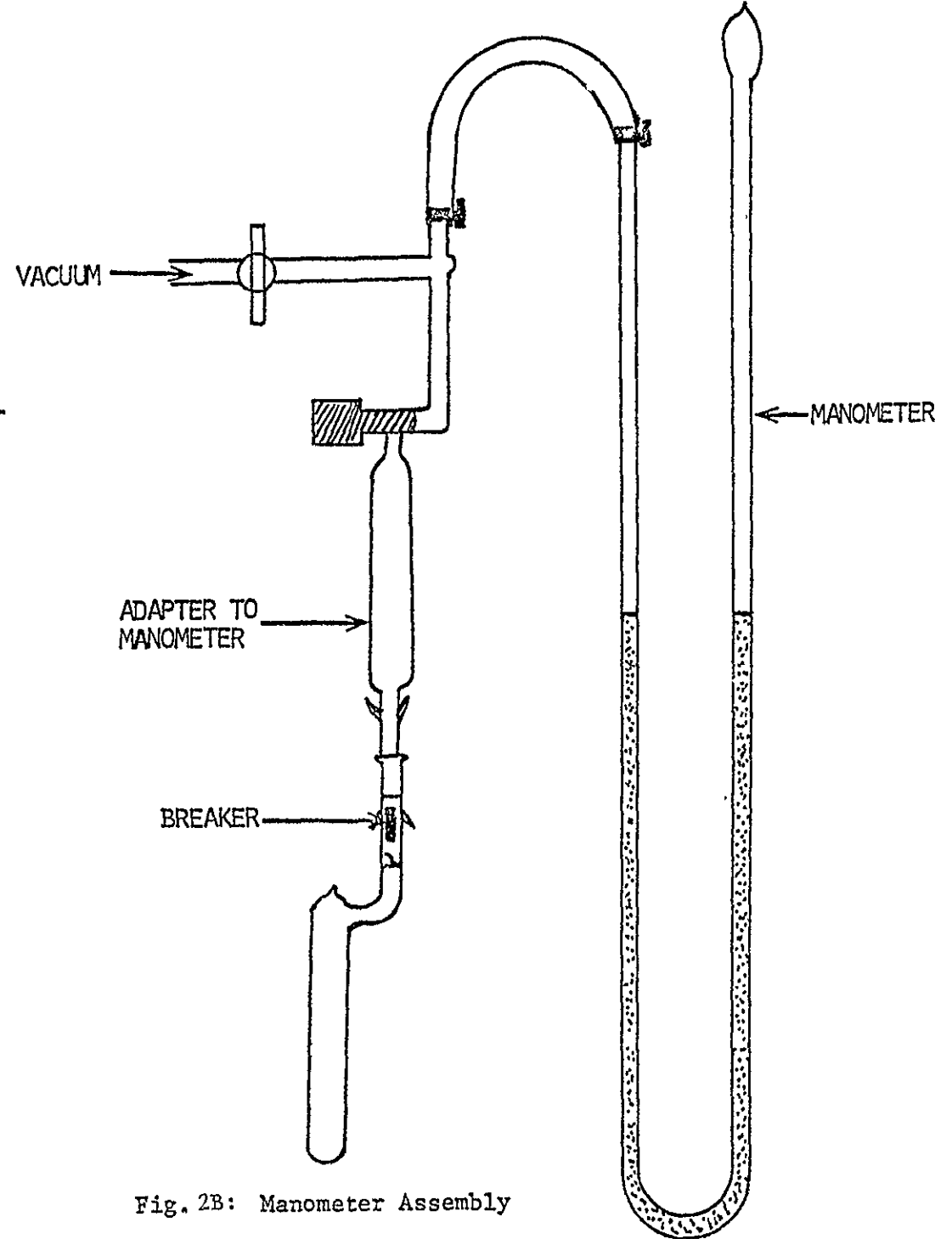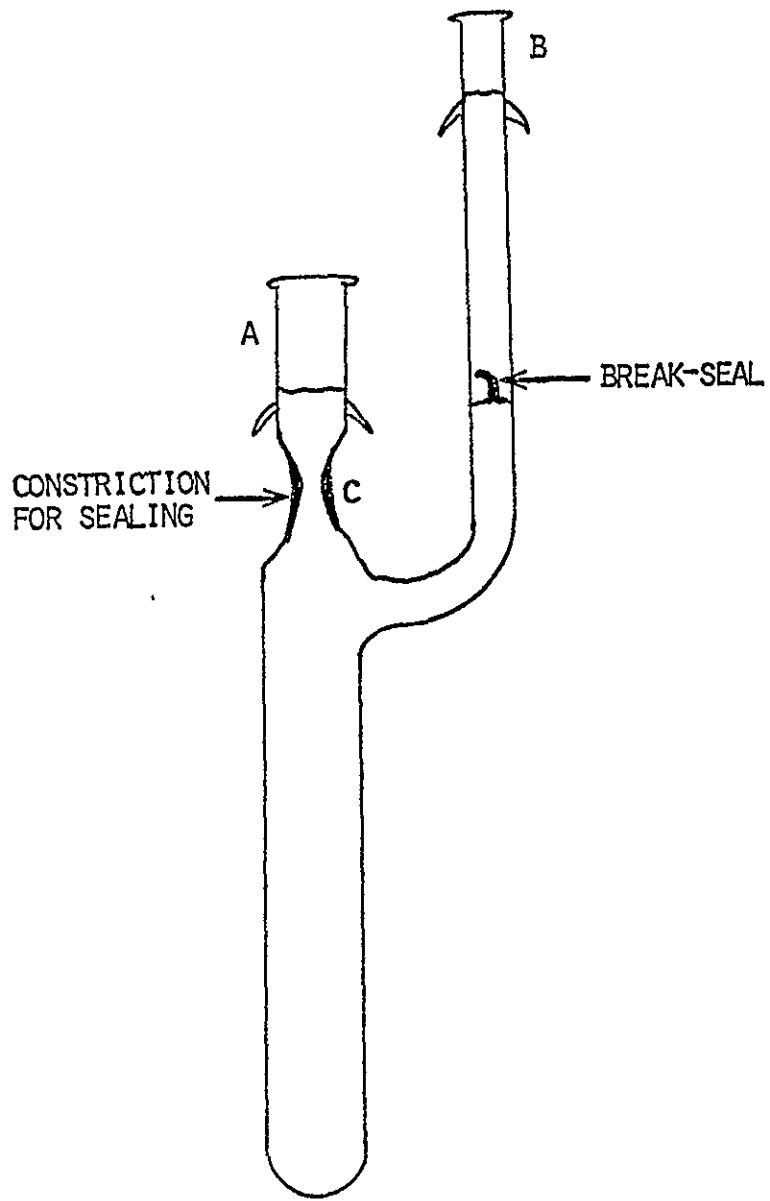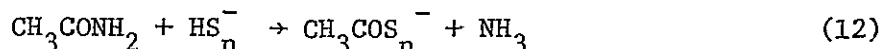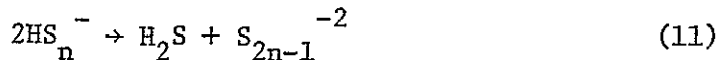
12

Fig. 2A: Sample tube for stability test.

Fig. 2B: Manometer Assembly

Thus no gases were formed from any of these amides. The IR and UV visible spectra of these solvents after the heat treatment did not show any noticeable changes. The results suggest that the overall thermal stabilities of the amides in the operating temperature range of the battery are satisfactory.

Stabilities of Amide/Na$_2$S Solutions. The test mixtures used for the evaluation are shown in Tables 3, 4, 5 and 6 respectively for the amides AC, NMAC, DMAC and DEAC. The monosulfide is only sparingly soluble in DMAC or DEAC. However, the results of tests, performed with an excess of undissolved Na$_2$S, indicated that these two amides are stable in the presence of Na$_2$S for at least 21 days at 130°C. No gases were produced from either the DMAC/Na$_2$S or the DEAC/Na$_2$S mixture. The solution maintained its colorless nature during the 21 days of heating. The visible-UV absorption spectra of DMAC or DMAC/Na$_2$S solutions recorded before and after heating are shown in Figure 3. The solutions heated for $\geq$ 6 days showed two absorption peaks at 285 nm and at 345 nm in addition to the peak at 265 nm due to DMAC. The peak at 285 nm is due to S^{-2}, as evidenced by the spectrum of a freshly prepared solution* of Na$_2$S in DMAC. A similar absorption pattern at ~280 nm is exhibited by a solution of Na$_2$S in DMF (16). The absorption peak at 345 nm is due to a reaction product. However, the intensity of the peak at 345 did not increase with increasing heating time, and the relative concentration of the material exhibiting this absorption was very small. Similar experiments with DEAC/Na$_2$S mixtures indicated that its stability was similar to that of the DMAC/Na$_2$S mixture.

The monosulfide was moderately soluble in the amides NMAC or AC at 130°C (see Table 3). The stability characteristics of the AC/Na$_2$S solution was investigated in detail. A mixture containing 0.33g (4.2 mmoles) Na$_2$S in 2.05g AC produced 1.01 mmoles of gases in 18 days at 130°C. Vapor phase IR spectrometry (Fig. 4) indicated the gases to be mostly NH$_3$. However, it contained small amounts of H$_2$S also. The formation of these products may be explained by the following general reactions in a solution of Na$_2$S$_n$ in acetamide

$$CH_3CONH_2 + S_n^{-2} \rightarrow CH_3CONH^- + HS_n^- \tag{8}$$

$$CH_3CONH_2 + HS_n^- \rightarrow CH_3CONH^- + H_2S_n \tag{9}$$

$$H_2S_n \rightarrow H_2S + (n-1)\ S° \tag{10}$$

$$2HS_n^- \rightarrow H_2S + S_{2n-1}^{-2} \tag{11}$$

$$CH_3CONH_2 + HS_n^- \rightarrow CH_3COS_n^- + NH_3 \tag{12}$$

---
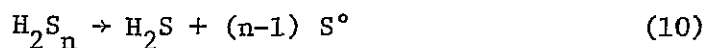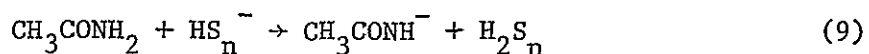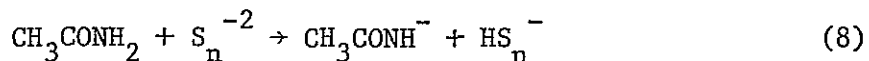
*The solution was obtained by heating an excess of Na$_2$S in DMAC for ~15 min at 80°C and subsequently cooling the solution to room temperature.

TABLE 3

STABILITY TEST DATA FOR ACETAMIDE/Na_2S_n MIXTURES AT 130°C

Tube No.	Reactants	No. of Days Heated at 130°C	mmoles of Gas	Comments
3A	2.02g AC, 0.21g Na_2S_9 (5.8 mmoles S)	5.5	2.75	Strong H_2S odor for gas. Strong onion odor for residue. New peak in the iR spectrum of solid at 2050 cm^{-1}. Vapor phase IR showed that the gas contained COS as a product.
3B	1.96g AC, 0.2228g Na_2S_8 (5.9 mmoles S)	12.0	3.50	Same as above.
3C	1.98g AC, 0.251g $Na_2S_{9.5}$	20.0	4.19	Same as above.
2A	2.01g AC, 0.239g Na_2S_4 (5.5 mmoles S)	5.5	0.22	Slight onion odor for residue. Strong H_2S odor for gas. COS as the major product in the gas by IR.
2B	1.998g AC, 0.228g Na_2S_4 (5.25 mmoles S)	13.0	1.02	Strong onion odor for residue. Strong H_2S odor for gas. Growth of new iR peak at 2050 cm^{-1}. Mostly COS in the gas as shown by vapor phase IR.
2C	1.966g AC, 0.253g Na_2S_4 (5.8 mmoles S)	21.0	0.58	Same as above.
4	2.05g AC, 0.328g Na_2S (4.2 mmoles S)	18.0	1.01	Solution turned dark brown from clear. The gas formed a green precipitate with $CuCl_2$. IR spectra showed it to be NH_3.
6A	1.953g AC, 0.2664g Na_2S_4 (6.12 mmoles S), 1.4M butylborate	11.0	–	Tube leaked.
6B	1.9622g AC, 0.2572g Na_2S_4 (5.91 mmoles S), 2.5M butylborate	11.0	0.42	Dark brown solution, appeared to be more viscous. The gas was found to be H_2S, COS and other minor components.

TABLE 4

STABILITY TEST DATA FOR NMAC/Na_2S_n MIXTURES AT 130°C

Tube No.	Reactants	No. of Days Heated at 130°C	mmoles of Gas	Comments
5A	1.982g NMAC, 0.1876g $Na_2S_{6.2}$ (4.86 mmoles S)	6	0.14	Dark red solution; gas was found to contain COS, H_2S and other minor products.
5B	1.879g NMAC, 0.1744g Na_2S_7 (4.63 mmoles S)	12	0.58	Same as above.
5C	1.85g NMAC, 0.1974g $Na_2S_{6.5}$ (5.16 mmoles S)	18	1.05	Same as above.

TABLE 5

STABILITY TEST DATA FOR DIMETHYLACETAMIDE/Na_2S_n MIXTURES AT $130°C$

Tube No.	Reactants	No. of Days Heated at 130°C	mmoles of Gas	No. of Moles of Gas/ Mole S	Comments
1A	2 ml DMAC, 0.207g Na_2S_4 (4.76 mmoles S)	5	0	-	All the Na_2S_4 dissolved and the solution had a green color.
1B	2 ml DMAC, 0.2161g Na_2S_4 (4.97 mmoles S)	12	0.01	-	Same as above.
1C	2 ml DMAC, 0.2440g Na_2S_4 (4.92 mmoles S)	21	0.01	-	Same as above.
2A	2 ml DMAC, 0.247g Na_2S_9 (6.64 mmoles S)	5	0.36	0.054	Solution was dark red. Major component in this gas phase was COS.
2B	2 ml DMAC, 0.2259g Na_2S_8 (5.942 mmoles S)	12	0.47	0.079	Dark red solution with green tinge at 130°C. Mostly COS in the gas.
2C	2 ml DMAC, 0.243g Na_2S_8 (6.472 mmoles S)	21	1.02	0.157	Green solution at 130°C became dark red on cooling. Mostly COS in the gas.
3A	2 ml DMAC, 0.344g Na_2S (4.4 mmoles S)	5	0	-	Very little Na_2S dissolved. The solution was clear.
3B	2 ml DMAC, 0.329g Na_2S (4.22 mmoles S)	12	0	-	Very little Na_2S dissolved. The solution was clear.
3C	2 ml DMAC, 0.319g Na_2S (4.10 mmoles S)	21	0	-	Very little Na_2S dissolved. The solution was clear.
3D	2 ml DMAC, 011g S (3.1 mmoles)	21	0.775	0.25	Yellow solution. The gases were a mixture of COS and CS_2 as evidenced by IR and mass spectra.

TABLE 6

STABILITY TEST DATA FOR DEAC/Na_2S_n MIXTURES AT 130°C

Tube No.		No. of Days at 130°C	mmoles of gas	% Sulfur Reacted	Comments
L_1	2 ml DEAC, 0.2671g $Na_2S_{7.3}$ (6.98 mmoles S)	7	0.686	9.8	Dark olive-green with brown tint.
L_2	2 ml DEAC, 0.243g $Na_2S_{7.5}$ (6.38 mmoles S)	14	0.739	11.6	Dark green solution at temperature. Turns dark brown on cooling.
L_3	2 ml DEAC, 0.2450g $Na_2S_{7.3}$ (6.46 mmoles S)	21	1.00	15.5	Same as above.
X_1	2 ml DEAC, 0.2305g Na_2S_4 (5.30 mmoles S)	7	0	–	Dark blue-green solution. Na_2S_4 not all dissolved.
X_2	2 ml DEAC, 0.2332g Na_2S_4 (5.36 mmoles S)	14	0	–	Same as above.
X_3	2 ml DEAC, 0.2542g Na_2S_4 (5.84 mmoles S)	21	0	–	Same as above.
C_1	2 ml DEAC, 0.2239g Na_2S (2.87 mmoles S)	6	0	–	Salmon color over Na_2S powder.
C_2	2 ml DEAC, 0.2120g Na_2S (2.72 mmoles S)	12	0	–	Same as above.
C_3	2 ml DEAC, 0.2227g Na_2S (2.86 mmoles S)	21	0	–	Same as above.
B	2 ml DEAC	21	0	–	Remained clear.
FF	2 ml DEAC + 0.13g S (4 mmoles)	43	0.53	13.25	Reddish-yellow solution.
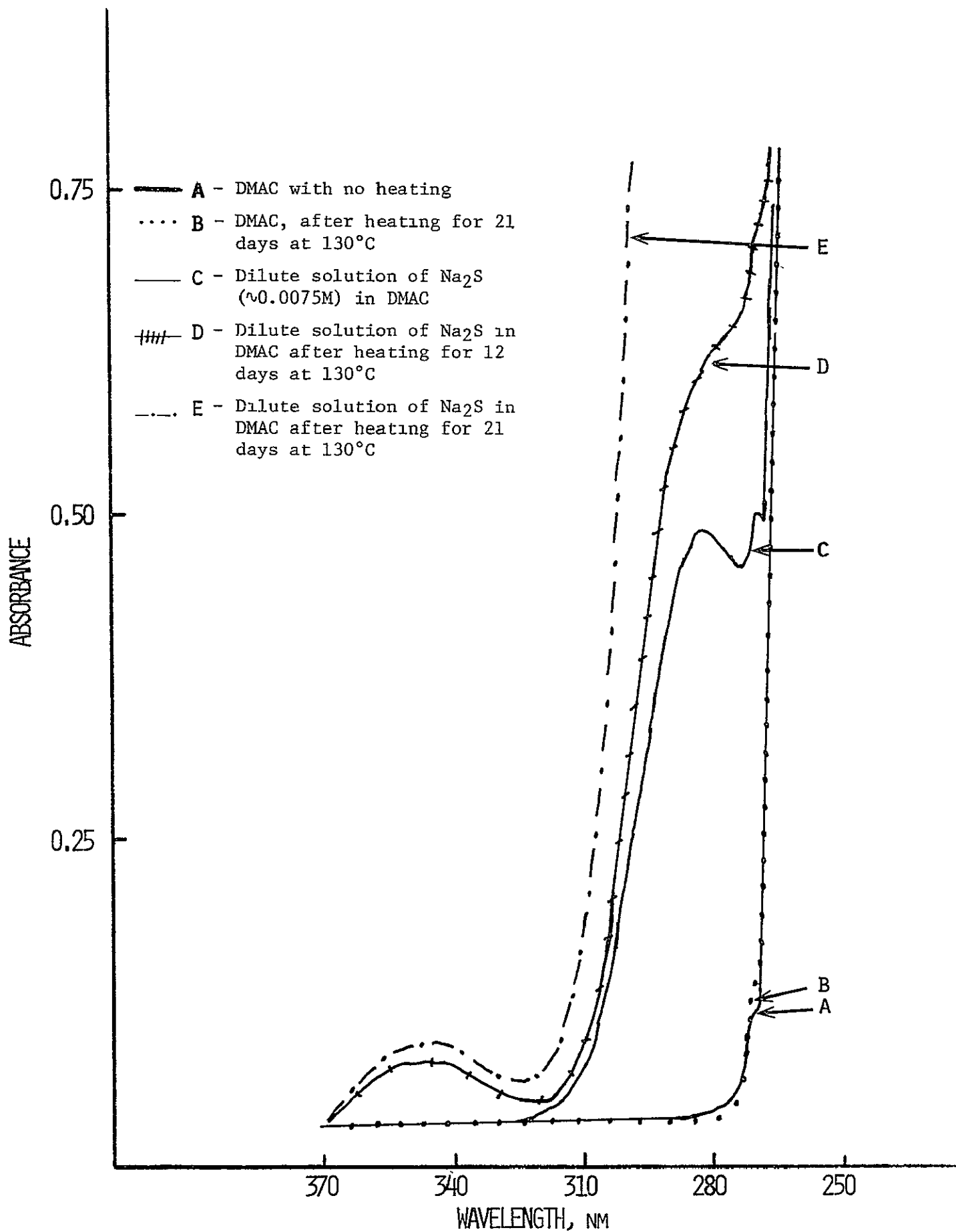
Fig. 3: Absorption spectra of DMAC or DMAC/Na2S solutions before and after heating at 130°C.

PERCENT TRANSMISSION

100

80

60

40

20

0

4000   3000   2000   1800   1600   1400   1200   1000   800   600   300
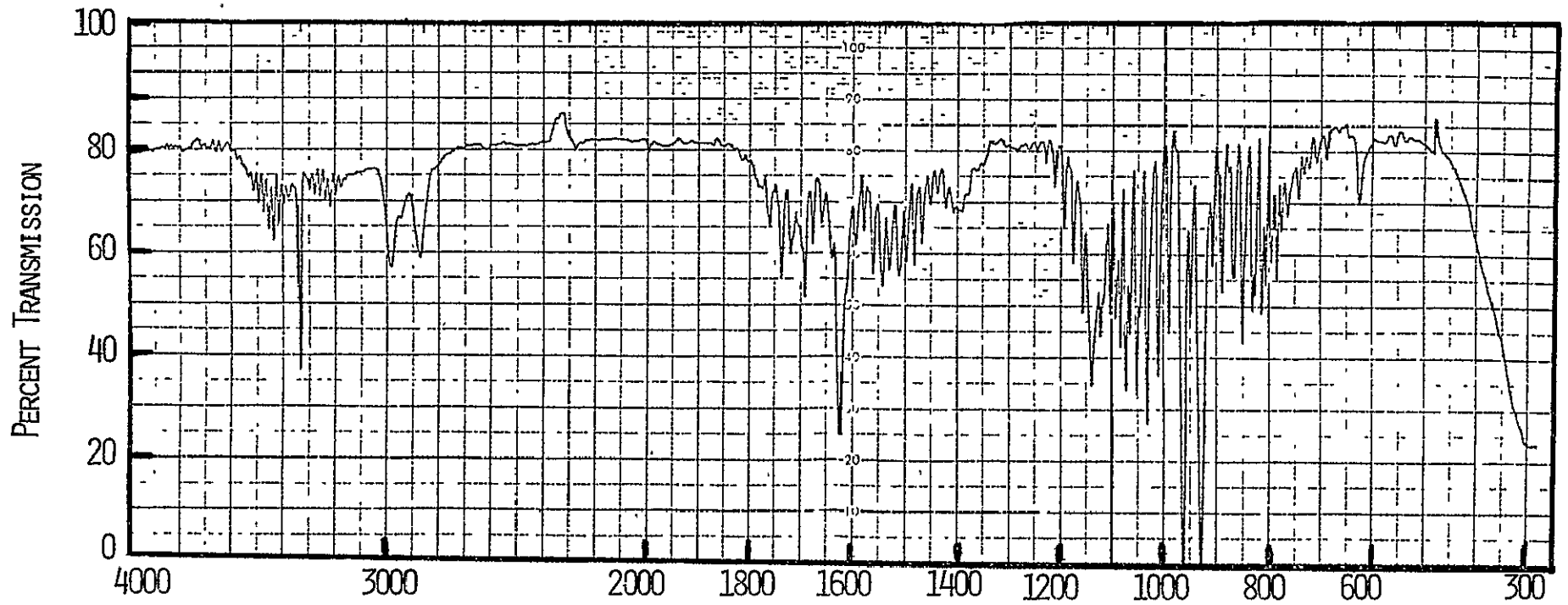
Fig. 4: Vapor phase IR spectrum of the gases from AC/Na_2S solution after 18 days of heating.

It appears that in an Na_2S/AC solution with an excess of acetamide, as in the present case, reactions 8 and 12 predominate. Reactions 9 and 11, leading to the formation of H_2S, probably occur only to a small extent. It may be noted that reaction 12 is analogous to the well characterized reaction of $CH_3COOC_6H_5$ with NaSH to form CH_3COSNa and C_6H_5OH, as depicted in Equation 13.

$$CH_3COOC_6H_5 + NaSH \rightarrow CH_3COSNa + C_6H_5OH \qquad (13)$$
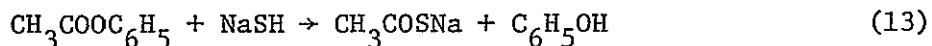
Stabilities of Amide/Na_2S_n, n > 1, Solutions. The tests were performed with amide/Na_2S_n solutions where n = 4 or ~8. The test solutions had a S concentration of ~2-3M/litre. The various test mixtures for the amides, AC, NMAC, DMAC and DEAC respectively are shown in Tables 3, 4, 5 and 6.

A solution of Na_2S_4 in DMAC or DEAC did not produce any gas even after heating for a period of 21 days at 130°C. The visible spectra of fresh and heated solutions, shown in Figure 5, were similar. The primary absorption in these solutions is the strong peak at 618 nm due to S_3^{-1}. The NMR and IR spectra also indicated no products in solution.

Longer-chain polysulfides (S_n^{-2}, n > 4), were found to react with DMAC or DEAC at 130°C. Both of these amides produced gases, the amount of which increased with increasing heating time. A plot of the amount of gases produced versus heating time (days) is shown in Figure 6. Vapor phase infrared spectrum (Fig. 7) indicated that the gases were the same from both of the amides and were identified as containing mostly carbon oxysulfide, COS. The visible spectra of these solutions also showed major changes after the heating. This is illustrated in Figure 8 for a solution of Na_2S_8 in DMAC. After heating for 21 days at 130°C, the absorption peak at 520 nm, characteristic of long chain polysulfides found in freshly prepared solution, has considerably decreased in intensity. The spectral properties of the solution before and after the heating suggest that during heating S° present in solution in equilibrium with polysulfides reacts gradually with the amides to produce carbon oxysulfide and polysulfides of shorter chain lengths. It appears, thus, that the reactive species in these solutions is elemental S. The stability tests at 130°C on mixtures of S and DMAC or DEAC seem to support this. Elemental S is insoluble in N,N-dimethylacetamide or in N,N-diethylacetamide at room temperature. However, when a mixture of S and either of these amides is heated to 130°C, an orange-yellow solution is formed. No gas is formed from this reaction mixture in 16 hr at this temperature. The visible spectra* of these solutions, Figs. 9 and 10, show broad absorptions with a peak at 437 nm for the DMAC-sulfur reaction product and two peaks at 500 nm and 425 nm for the DEAC-sulfur reaction product.

---

*The solvents alone show no absorptions above 300 nm after heating for the same period of time.
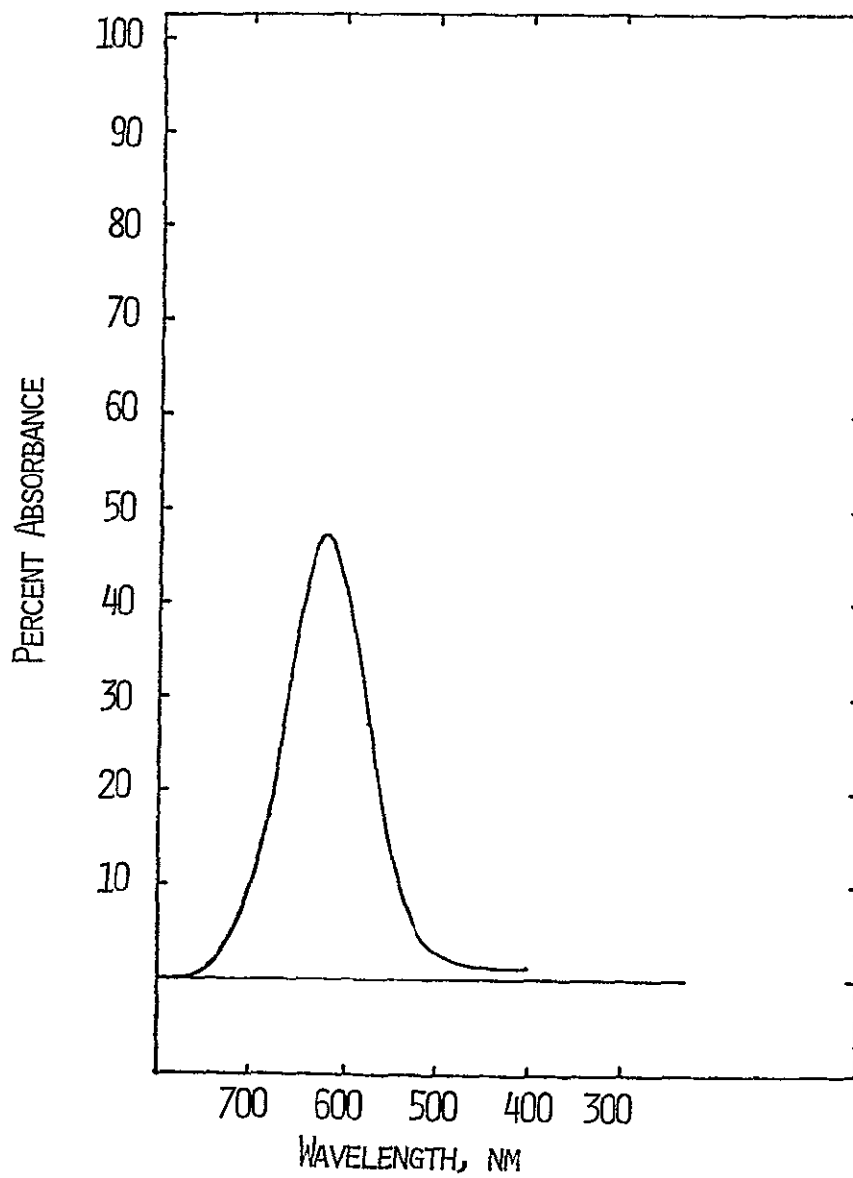
Fig. 5: Visible spectrum of a solution of Na_2S_n in
DMAC after heating for 21 days at 130°C.
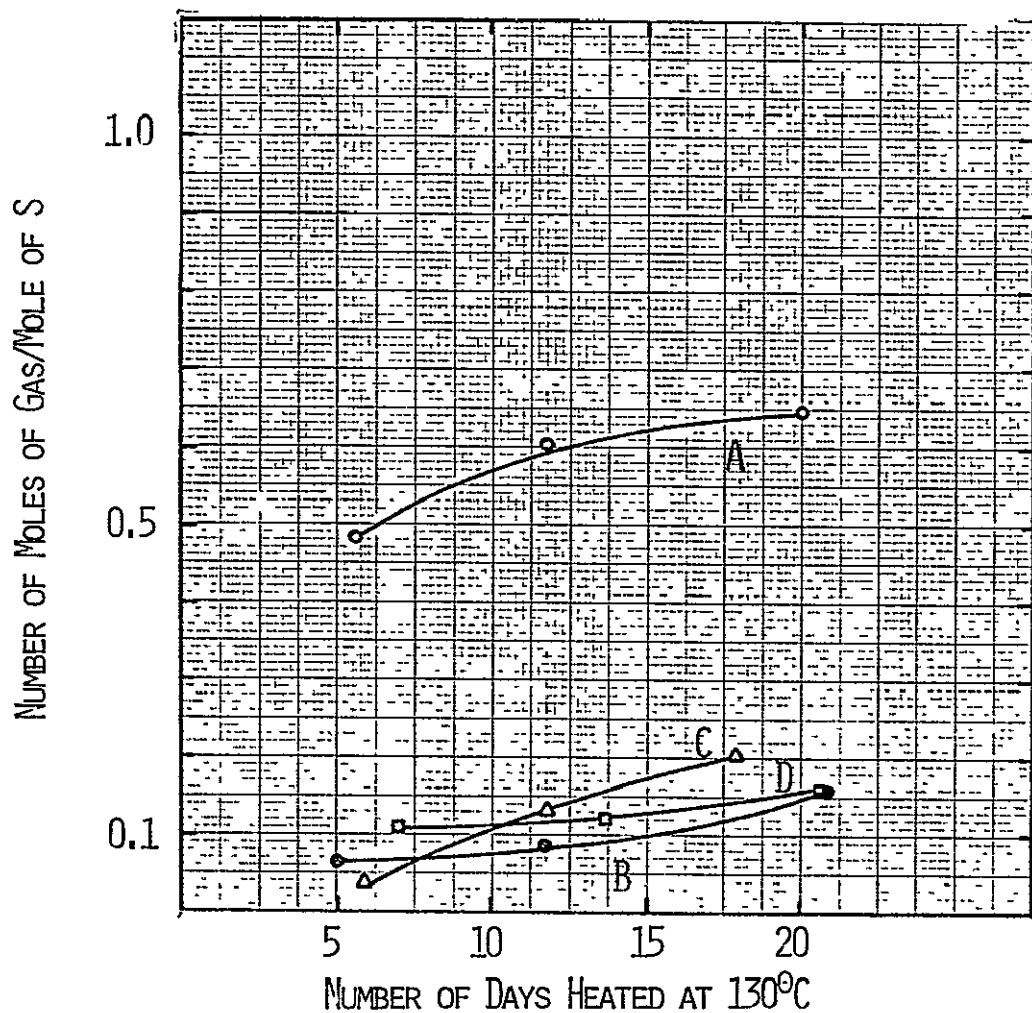
Fig. 6: A plot of the amount of gas produced vs. heating time for amide/Na_2S_n solutions

A – AC/Na_2S_n solution, n = 8
B – DMAC/Na_2S_n solution, n = 8
C – NMAC/Na_2S_n solution, n = 6
D – DEAC/Na_2S_n solution, n = 8

WAVELENGTH IN MICRONS

WAVENUMBER, cm^{-1}
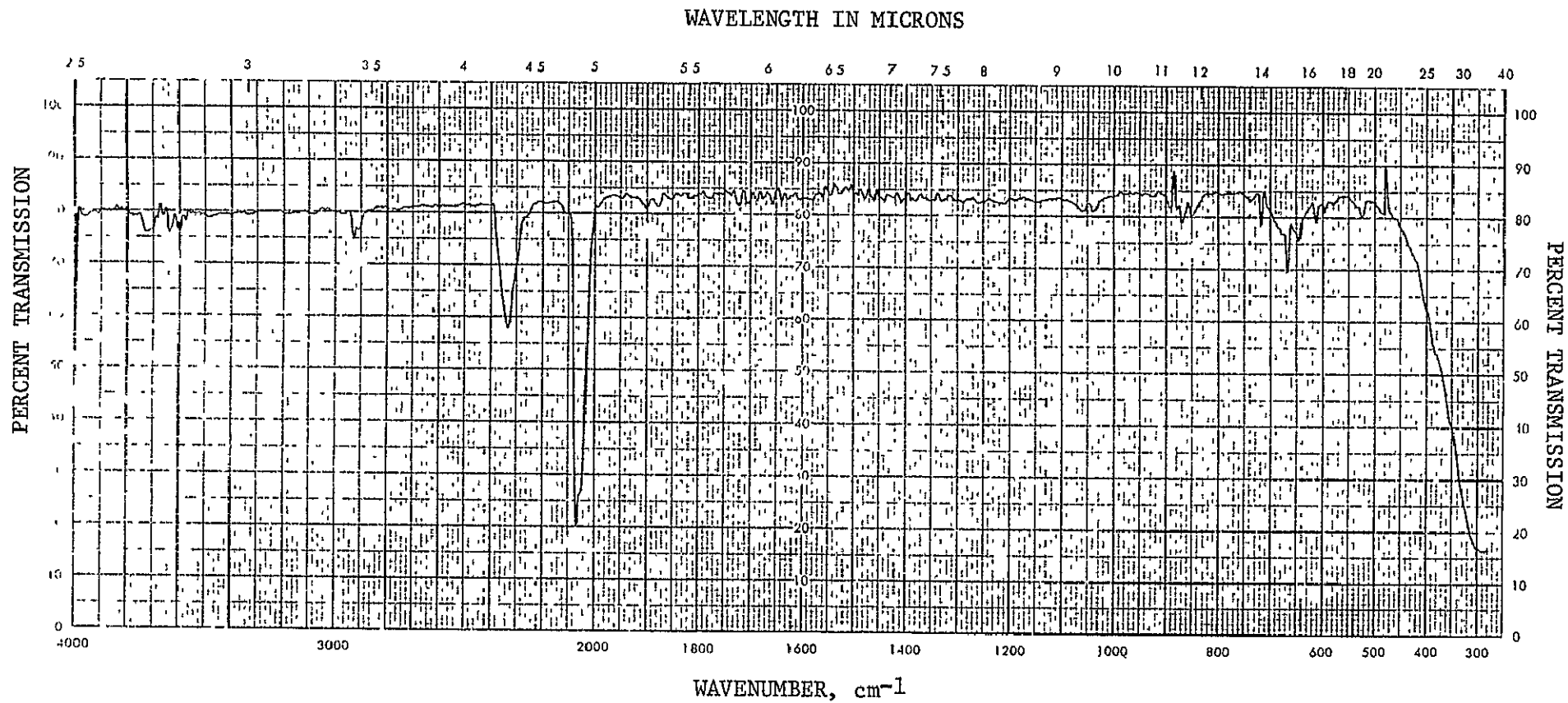
Fig. 7: Vapor phase infrared spectrum of gases from DMAC/Na$_2$S$_8$ solution after 21 days of heating at 130°C.

24
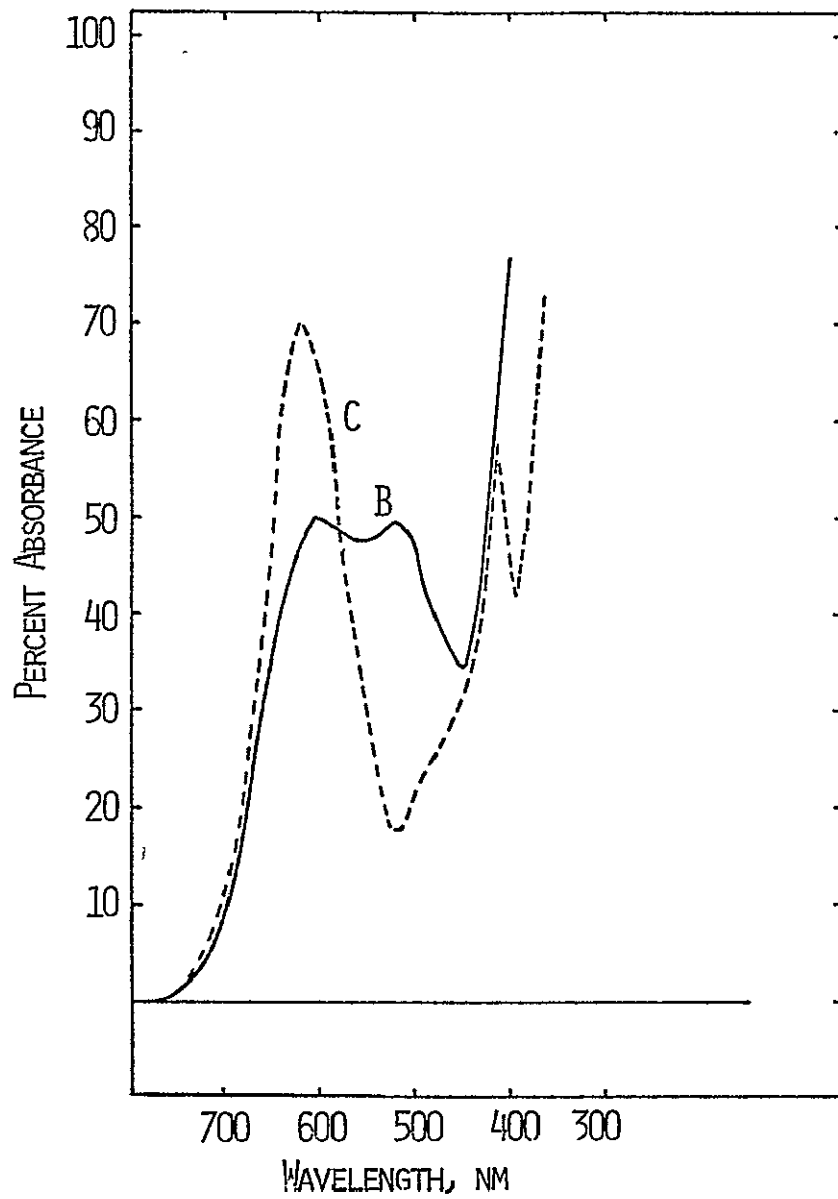
Fig. 8: Visible spectra of solutions of Na_2S_8 in DMAC.

B – After heating for 12 days at 130°C
C – After heating for 21 days at 130°C

Fig. 9: Visible absorption spectra of 1M DEAC/S reaction
product in solution.

A - after 16 hours of heating at 130°C
B - After 40 days of heating at 130°C

Fig. 10: Visible absorption spectra of the DMAC/S
reaction product in solution.

A — after 16 hours of heating at 130°C
B — After 21 days of heating at 130°C

Further heating of these solutions produce gases, the amount of which increases with increasing heating time. Some changes are also observed in the visible spectrum of the solution, although the gross features of the spectra are maintained. Vapor phase infrared (Fig. 11) and mass (Fig. 12) spectral data proved that the gases were a mixture of carbon oxysulfide (COS) and carbon disulfide (CS_2). About 75% of the mixture was carbon oxysulfide. It was found that the reaction of each of the four amides with S under the present reaction conditions produces a similar mixture of volatile products of COS and CS_2. The evidence that COS and CS_2 are produced considerably after the initial reaction with S, suggests that in all cases these gases are secondary reaction products. It appears that elemental sulfur reacts initially with the amides to produce long chain sulfur containing products which on continued heating decomposes to give COS and CS_2, as shown in Equations 14 and 15.

$$CH_3CON(CH_3)_2 + nS \xrightarrow{130°C} CH_3COS_nN(CH_3)_2 \qquad (14)$$

$$I$$

$$CH_3COS_nN(CH_3)_2 \xrightarrow{\Delta} CH_3S_{n-1}N(CH_3)_2 + COS \qquad (15)$$
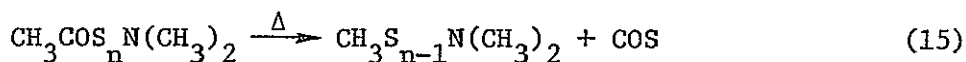
$$II$$

The various physical properties of the solution products are also consistent with the formation of the polysulfides I and II. For example, the visible spectrum resembles that of alkali metal polysulfides in non-aqueous solvents (10). The infrared spectrum of the orange solution from DMAC and S exhibited an absorption at 1135 cm^{-1} which is in the region of C-S stretching vibrations. The ^{1}H NMR spectrum of this solution exhibited a complex pattern. Nevertheless, the presence of new $-N(CH_3)_2$ resonances centered at 2.9 ppm and a new-$COCH_3$ or $-SCH_3$ resonance at 1.51 ppm, are also consistent with the structures I and II.

The formation of the same gas products from the reactions of both elemental S and Na_2S_n, n > 4, suggests a possible explanation for the observed reaction with Na_2S_n, n > 4 as follows:

A variety of equilibria involving S chains and elemental S are usually present in solutions of alkali metal polysulfides in nonaqueous solvents. There is evidence, from spectroscopic and electrochemical studies (17), for the existence of equilibrium of the type 16, in solutions of alkali metal polysulfides in solvents such as dimethylsulfoxide (DMSO) or tetrahydrofuran (THF).

$$S_n^{-2} \rightleftharpoons S_{n-x}^{-2} + xS° \qquad (16)$$

WAVELENGTH IN MICRONS

WAVENUMBER, cm^{-1}

Fig. 11: Vapor phase infrared spectrum of the gases from DMAC/S solution after 21 days of heating at 130°C.

29
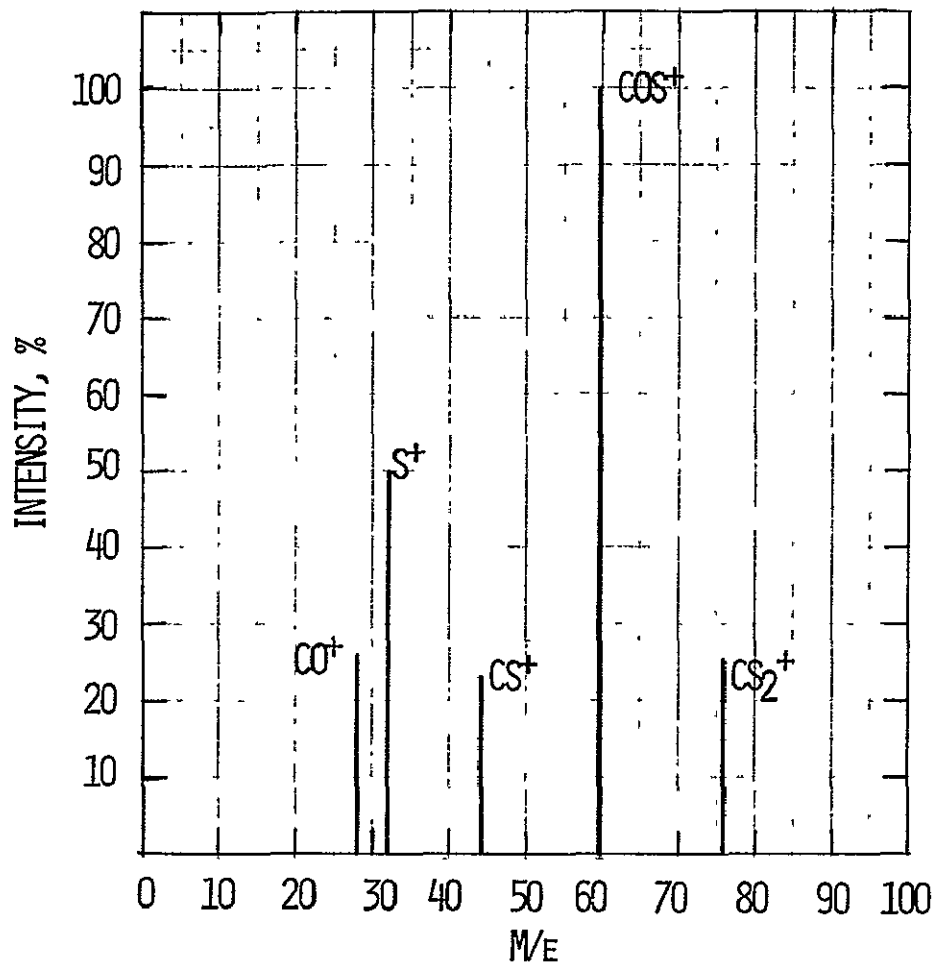
Fig. 12:   Mass spectrum of the gases from DMAC/S solution
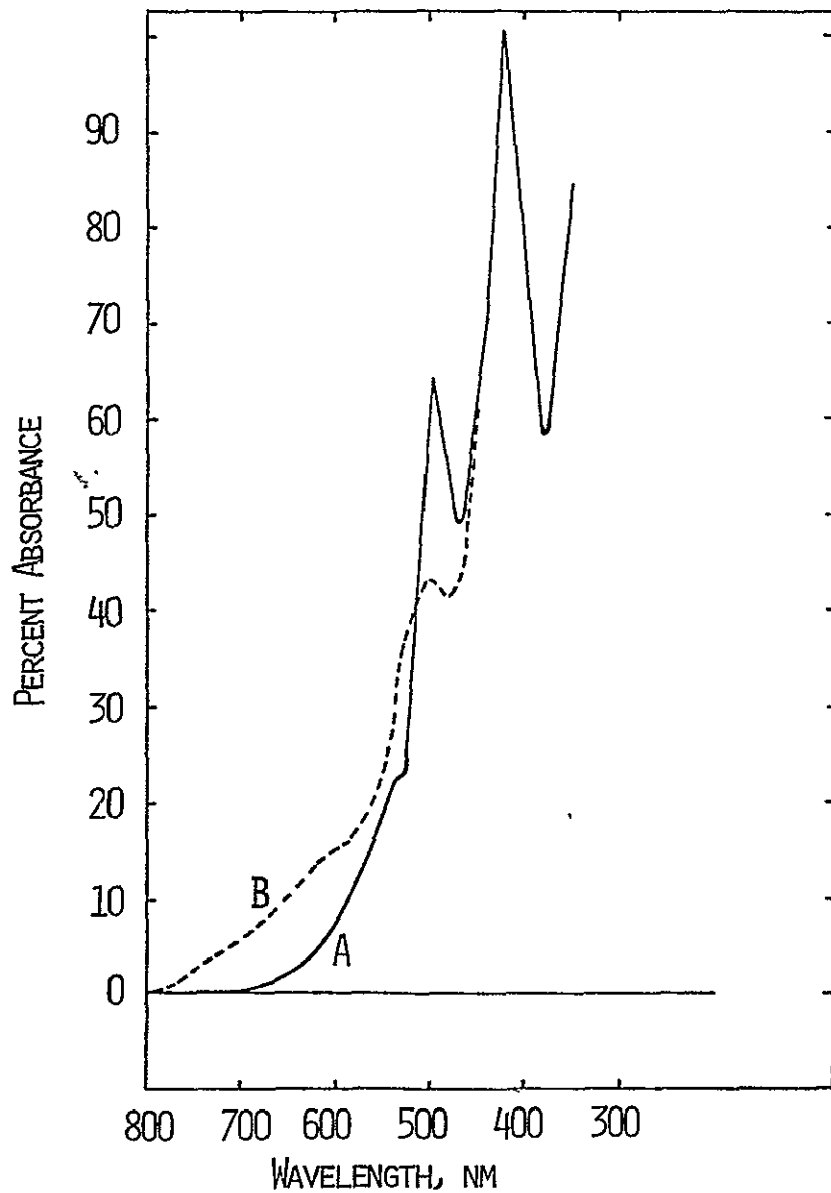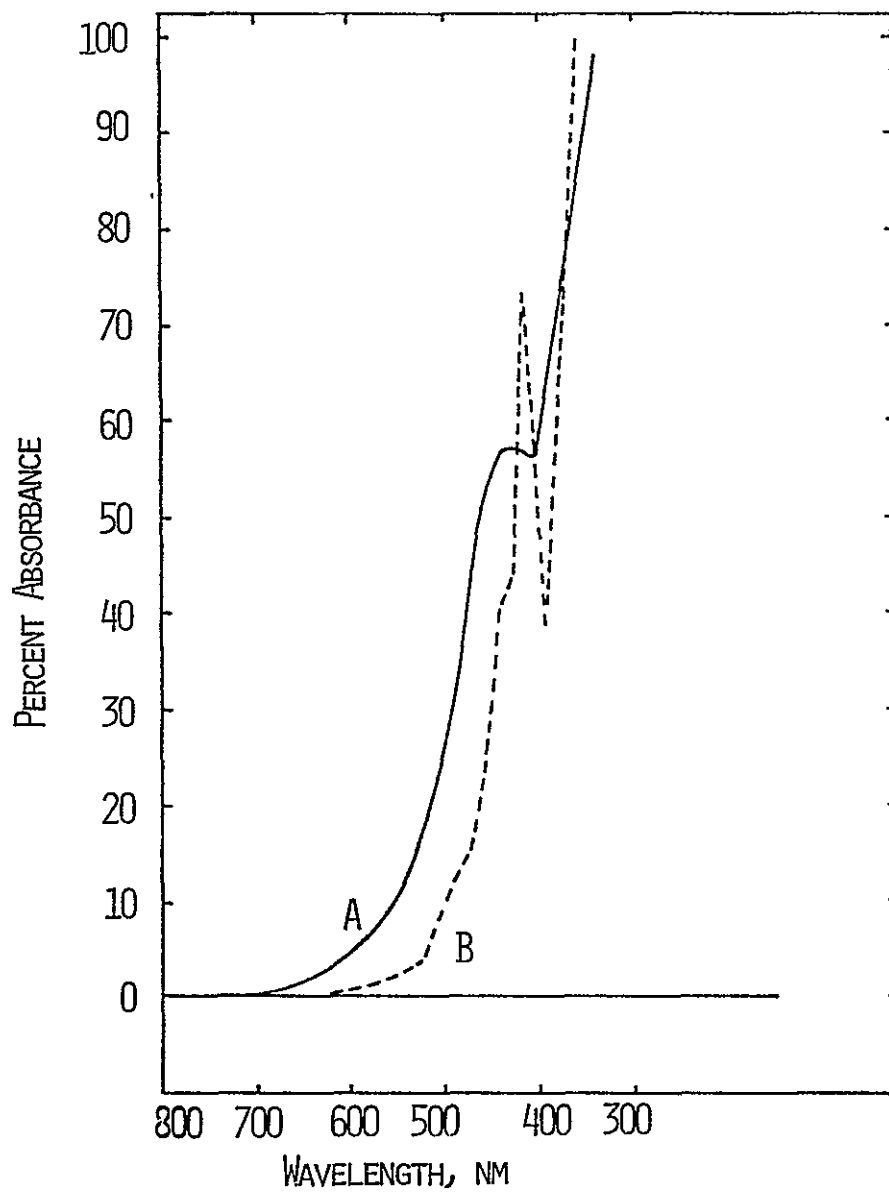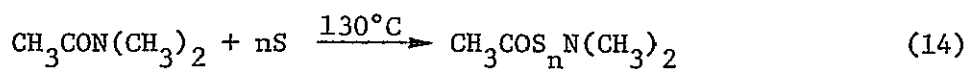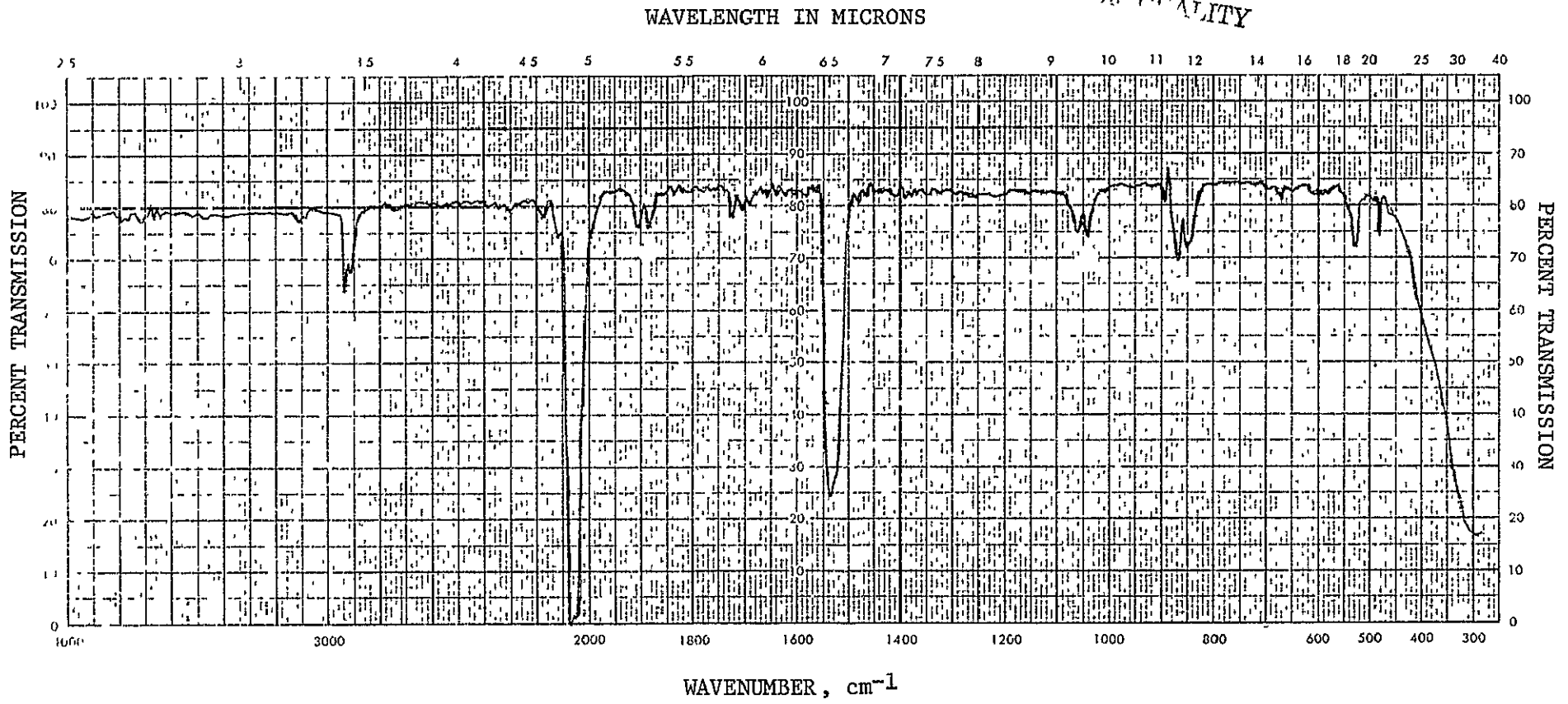after 21 days of heating at 130°C.

The solution properties of S_n^{-2} in DMAC resemble strongly those of S_n^{-2} in DMSO (17). It appears that when a solution of S_n^{-2}, n > 4, in DMAC, is heated, the neutral S present in equilibrium, reacts with the amide to form I. This reaction shifts equilibrium 3 to the right until all the S_n^{-2} is converted to S_4^{-2}. Further dissociation of S_4^{-2} is not observed, probably because of a unique stabilization of S_4^{-2} in this solvent. Spectral data suggest that S_4^{-2} is strongly dissociated in DMAC to form S_3^-, according to Equation 17.

$$2S_4^{-2} \rightarrow S_2^{-2} + 2S_3^-$$ (17)

In general, it is seen that basic solvents such as DMAC, DEAC, hexamethyl phosphoramide (HMP) or DMSO promotes the dissociation of S_4^{-2} in the manner shown in Equation 17. The rather high concentration of the anion radical in these solvents may indicate a unique stabilization accorded to it through solvent coordination. A common feature of all these solvents is that they possess electron-rich structural units such as C=O, P=O, or S=O. It appears that the solvent-S_3^- coordination occurs through these functional groups and may involve a five-membered ring structure, III.

III.
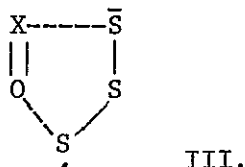
Solutions of S_n^{-2}, n > 4, in acetamide or N-methylacetamide also behave in a similar manner to the N-dialkyl substituted amides, except that the acetamide solution is much less stable. Some H_2S is also produced from these solutions. The formation of H_2S may be explained on the basis of Equations 8-11.

● Summary and Conclusion of Stability Studies

The aliphatic amides investigated in this program are thermally stable for long periods of time in the temperature range of 100 to 150°C. However, their Na sulfide solutions show varying degrees of reactivity which depend both on the nature of the sulfide and the nature of the amide. The overall stability trend is $CH_3CON(CH_3)_2 \approx CH_3CON(C_2H_5)_2 > CH_3CONH(CH_3)_2 \gg CH_3CONH_2$. It is also found that with the dialkyl substituted amides, the reaction is limited to Na_2S_n, with n > 4. Thus, of the four solvents the most suitable ones are $CH_3CON(CH_3)_2$ and $CH_3CON(C_2H_5)_2$. With these two solvents, it might be possible to achieve a relatively stable cathode by suitably controlling the charging limit of the battery to the formation of a medium chain polysulfide such as S_4^{-2}.

31

3. Sodium-Sulfur Cell Studies with CH_3CONR_2/Na_2S_n Cathodes

● Experimental Results

In a previous program (10), we studied the cycling behavior of the DMAC/Na_2S_n cathode, incorporated in a cell of configuration shown in Figure 13. During short-term cycling studies, this cell exhibited good reversibility between voltage limits of 1.00 and 2.70V. Typical discharge/charge curves are shown in Figure 14. The average cathode cycling stoichiometry at 130°C corresponded to

$$5S_2^{-2} \rightleftharpoons S_{10}^{-2} + 8e^- \tag{18}$$

No elemental S was formed during cell charging, but only long chain, soluble polysulfides. The major system limitation was found to be the termination of discharge (sharp voltage cutoff to 1.0V) in the vicinity of a polysulfide composition of S_2^{-2}. The major reasons for this appeared to be the very low solubilities of the lower order polysulfides and the consequent choking of the carbon felt current collector by the precipitated Na sulfide(s).

The carbon current collector in the above cells was fabricated from graphite felt (Union Carbide WDF felt). This has a porosity of only ∿15% (1). The Teflon-bonded carbon electrode used in Li/soluble S cells (17) or in Li/SOCl$_2$ cells (18) has a porosity in the neighborhood of 80%. The effect of the higher porosity Teflon-bonded carbon electrode on the discharge capacity of the DMAC/Na_2S_n cathode was assessed in the present study using a cell similar to the one shown in Figure 13, except that the graphite felt electrode was replaced with a Teflon-bonded carbon electrode. The latter electrode, 6 cm × 3.6 cm × 0.096 cm, was fabricated by Teflon-bonding 0.6g Shawinigan 50% compressed carbon black on an expanded stainless steel grid (Exmet Corp.) The electrode was wound around the β-Al_2O_3 tube and, when placed in the cell, it was firmly positioned by pressure contacting the walls of the two compartments. The cell was filled with 7 ml of 4M S as Na_2S_4 in DMAC/0.75M NaI electrolyte. The open circuit potential of the cell was 1.82V, as found previously with the graphite felt electrode, and the cell exhibited a resistance of ∿7Ω at 130°C. The cell was galvanostatically discharged and charged within the limits of 1.00 and 2.40 volts. A typical charge/discharge curve is shown in Figure 15. The open circuit potential of the cell, measured at the end of discharge was 1.23V. This suggests that the discharge of Na_2S_n to a composition below S_2^{-2} was achieved with the Teflon-bonded carbon electrode as opposed to a discharge only to S_2^{-2} with graphite felt. In the latter case, the OCV of the cell at the end of discharge, corresponding to the polysulfide composition of S_2^{-2}, was 1.76V. The present cell cycled five times, and the average
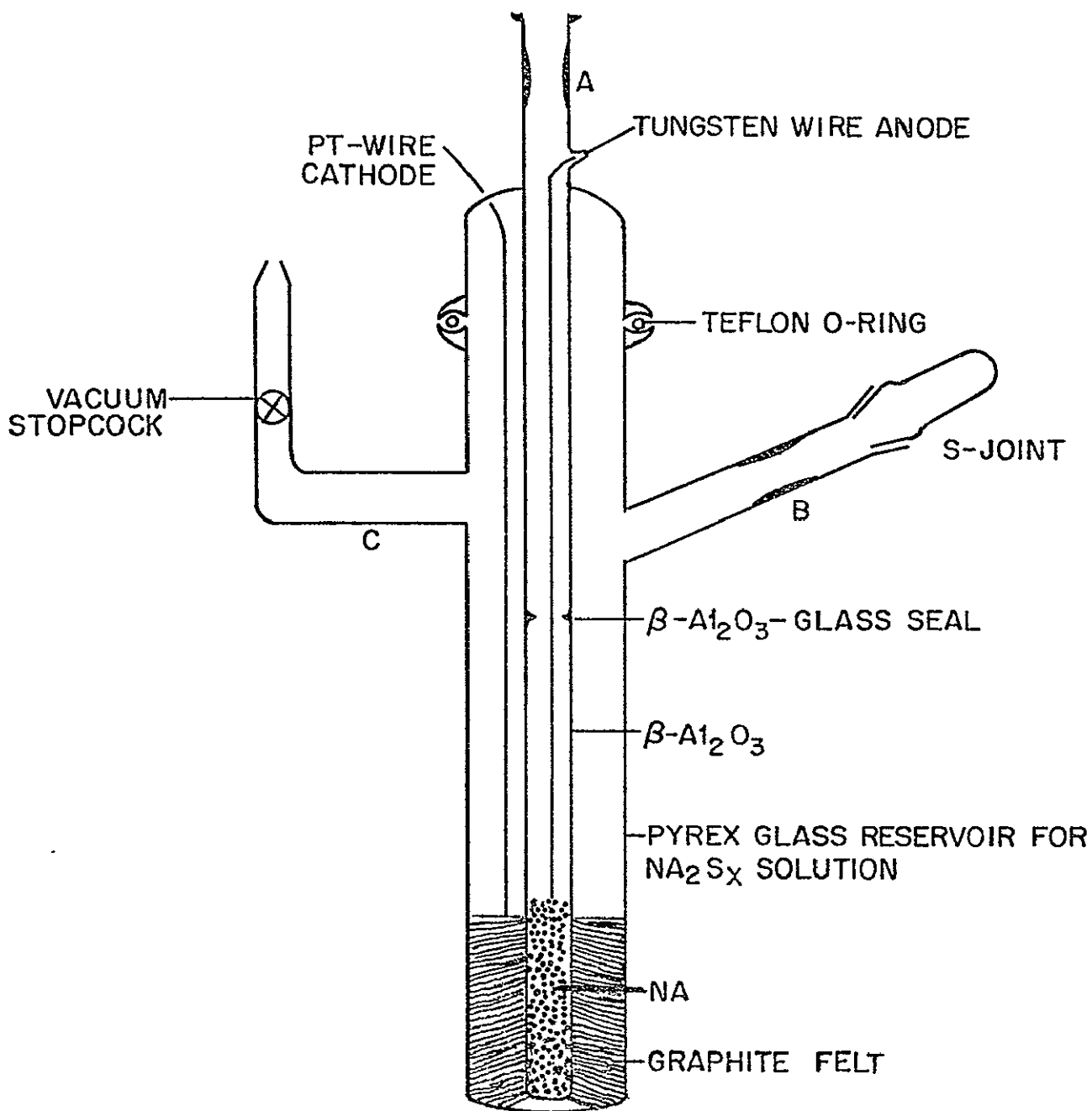
Fig. 13: High temperature electrolytic cell having a β-Al_2O_3 separator.
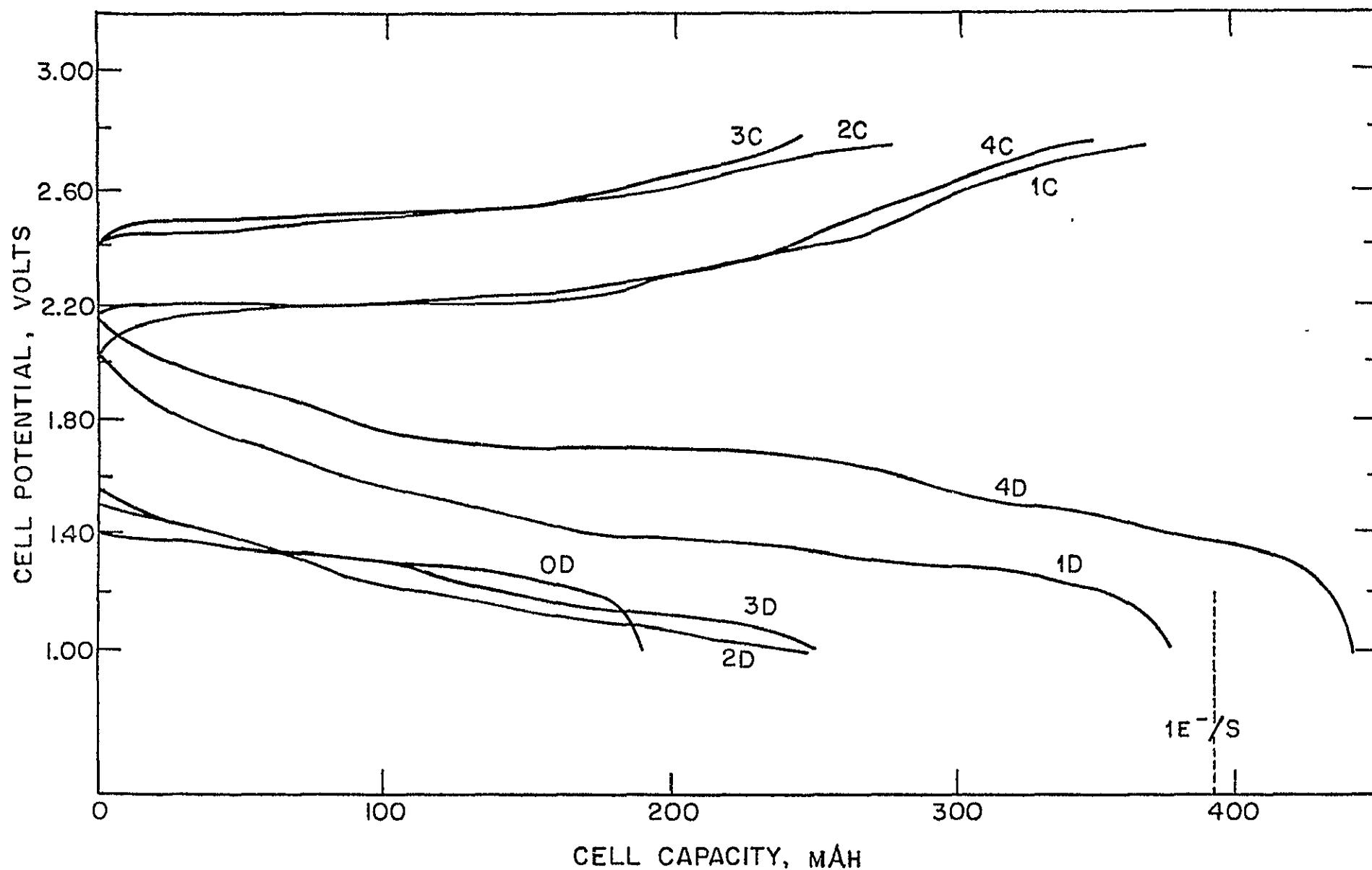
Fig. 14: Galvanostatic charge (C)/discharge (D) curves for a cell of configuration molten Na/β-Al$_2$O$_3$/Na$_2$S$_4$ (2.4M S) NaBF$_4$ (0. 4M), DMAC/carbon felt at 130°C. Current densities based on 12.6 cm^2 electrode area: 4C, 4D, 1.59 mA/cm^2; 1C, 1D, 2.4 mA/cm^2; OD, 2C, 2D, 3C, 3D, 3.2 mA/cm2.

34
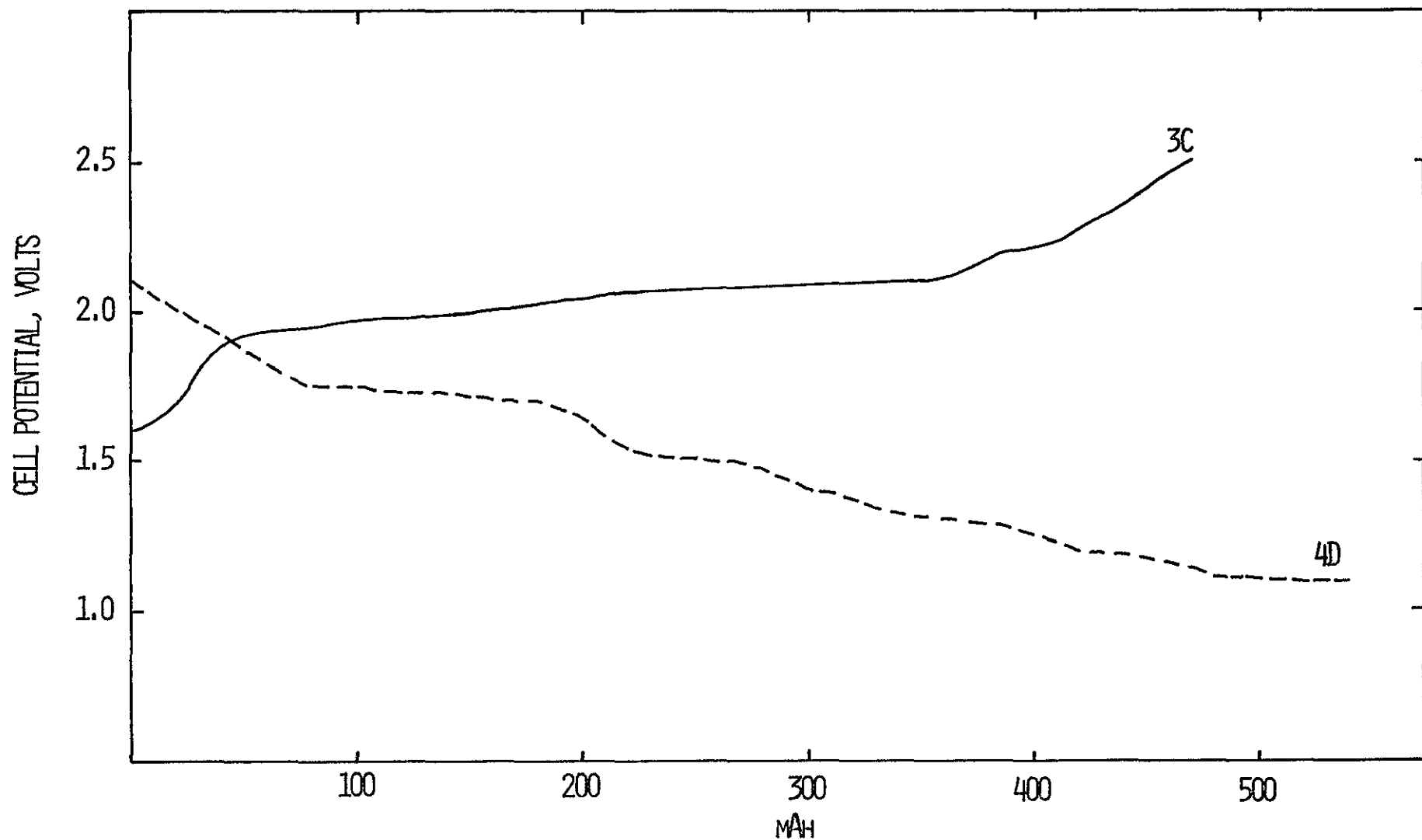
Fig. 15: The third discharge (3C) and fourth discharge (4D) curves for a cell, liquid Na/β-Al$_2$O$_3$/Na$_2$S$_4$ (4M S), 0.75M NaI, DMAC/Teflon-bonded C electrode at 130°C. ·Current = 20 mA; current density = 2 mA/cm^2. The cell was tested galvanostatically.

charge utilization in discharge was just below 1e⁻/S. However, the lower S utilization might be due to the unoptimized current collector, especially with respect to the solution to current collector volume ratio. Since we know that the primary self-discharge reaction is the reaction of the amide with elemental S, which would occur in significant amounts only when the polysulfide composition is >4, it might be possible to achieve long cycle life as well as good S utilization with an optimized cathode structure consisting of a solution of Na_2S_n in DMAC and a high porosity carbon such as a Teflon-bonded carbon current collector. Note that the reversible reaction

$$S_4^{-2} + 6e^- \rightleftarrows 4S^{-2} \tag{19}$$

involves 1.5e⁻/S, and the loss of ∿0.3e⁻/S by restricting the charging limit to S_4^{-2} is minor, compared with the possible gain in cycle life.

The cycling behavior of a Na/S cell with a DEAC/Na_2S_n/NaI cathode was also evaluated. A Teflon-bonded carbon electrode similar to the one discussed above was used. The cell initially contained 6 ml of a 2M S solution as Na_2S_4 in DEAC/0.5M NaI electrolyte. The OCV of the cell was initially 1.84V, similar to that observed with a DMAC/Na_2S_4 cathode. The cell exhibited a resistance at 130°C of 15Ω. The cell was cycled at the various constant currents of 10, 20 and 30 mA, corresponding to current densities of 1, 2 and 3 mA/cm². Cycling limits of 1.0V and 2.7V were used. The discharge/charge curves are shown in Figures 16, 17 and 18. The cell exhibited good reversibility behavior, although the discharge capacity did show a tendency to decrease with increasing cycle number, especially after the 5th discharge. Much of this loss may be attributed to the self-discharge reaction between DEAC and elemental S. In this cell, we made no attempt to restrict the charging limit to an intermediate size polysulfide chain such as S_4^{-2}, the highest charge composition with minimal amounts of elemental sulfur in equilibrium.

● Summary and Discussion of Cell Cycling Studies

The cell cycling studies indicate that DMAC and DEAC exhibit analogous behavior with respect to their solvent properties for the dissolved S cathode. The discharge capacities obtainable practically for cathodes consisting of solutions of Na_2S_n in these two solvents appear to be strongly dependent on the porosity of the current collector; the more porous the current collector, the greater the depth of discharge. This results from the fact that with a highly porous current collector, it would be possible to store larger amounts of the insoluble di- and monosodium sulfides on the electrodes, as is done in the case of Li/SOCl₂ cell (18). There is a slow self-discharge reaction in these cathode systems. However, it appears that this can be minimized greatly by restricting the charging

Fig. 16: Galvanostatic discharge/charge curves for a cell, liquid Na/β-Al$_2$O$_3$/Na$_2$S$_4$ (2M S), 0.5M NaI, DEAC/Teflon-bonded C electrode at 130°C. Current = 10 mA; current density = 1 mA/cm^2. Cell was discharged first, 1D. The charge curve 10C represents the last charge half cycle after the cycles shown in Figs. 17 and 18.
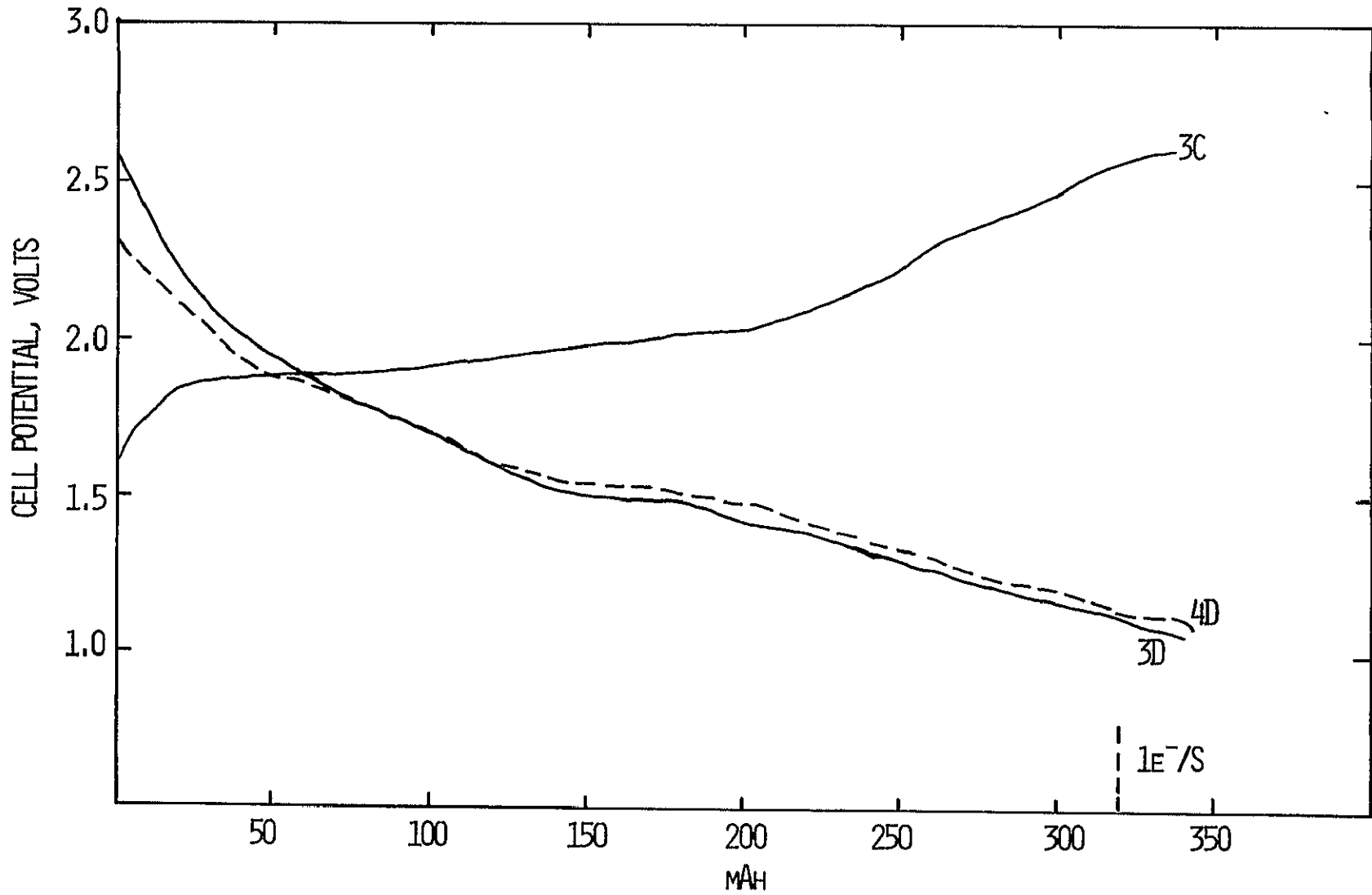
Fig. 17: The third discharge (3D), third charge (3C) and fourth discharge (4D) curves for the cell shown in Fig. 16. Current = 20 mA, current density = 2 mA/cm^2.
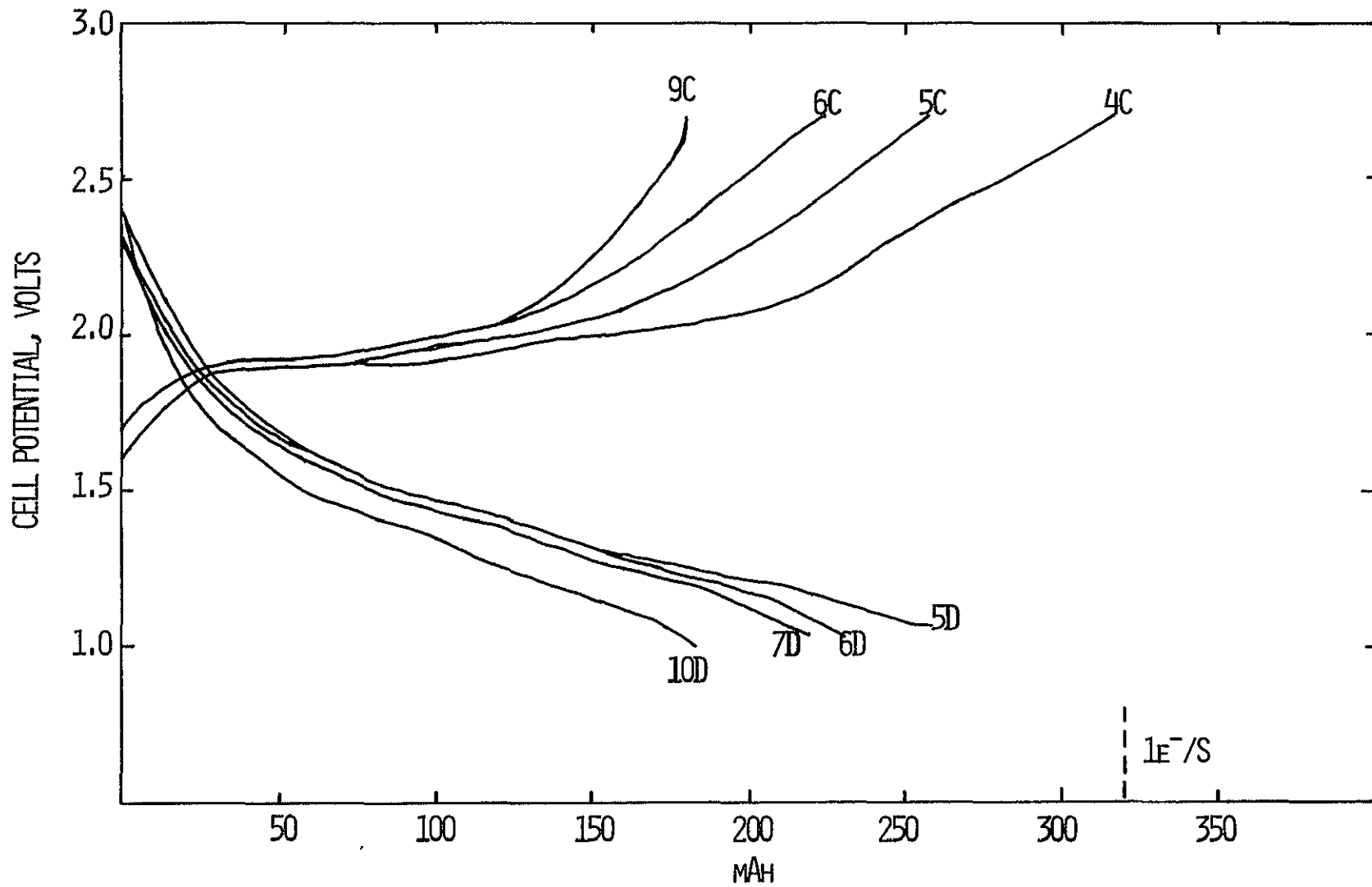
Fig. 18: Cycles five through ten of the cell shown in Fig. 16. The 7th and 8th charge and 8th and 9th discharge curves are not shown. Current = 30 mA, current density = 3 mA/cm^2.

limit of the battery to a medium size polysulfide such as S_4^{-2}. Comparison with the high temperature battery (1) shows that for an equivalent energy density of 60 Whr/lb, it is necessary to achieve a solubility (as Na_2S_{10}) of ∿1.3M if the charged cathode is to be in solution and if a complete reduction to S^{-2} is obtained. As we have seen, with a highly porous cathode it might not be necessary to achieve this much solubility for S_n^{-2}. The insoluble materials could be stored on the cathode current collector itself. To date only lower-rate cycling has been achieved, mostly due to ohmic drops in thick, non-state-of-the-art $\beta-Al_2O_3$ tubes.

B.   Sodium-Sulfur Cell with a 1,3 Cyclohexanediol (CHD)/Na_2S_n Cathode

Alcohols, in general, are unstable in the presence of Na_2S_n at temperatures >100°C. However, it was pointed out to us by Drs. W. L. Fielder and J. Singer of NASA-Lewis that 1,3 cyclohexanediol (CHD), $C_6H_{10}O_2$, was an exception. Long-term stability tests, carried out as in the case of the amide/Na_2S_n solutions, indicated that CHD/Na_2S or CHD/Na_2S_n, n = 4, 8, were stable at 130°C at least for 21 days. The higher stability of this diol may be associated with the "cyclohexane structure". Two cells were studied using this solvent. They were: (i) cell in which the initial catholyte was CHD/Na_2S/0.5M NaBr, (ii) cell in which the initial catholyte was CHD/Na_2S_4/0.5M NaBr.

1.   Cell with CHD/Na_2S/0.5M NaBr Solution as the Initial Catholyte

The cell was assembled, as described earlier. Since Na_2S is soluble in CHD to the extent of about 1M, the cell was initially charged with 1.1g of Na_2S and 7 ml of CHD/0.5M NaBr electrolyte was then added to make the solution the equivalent of ∿2M in Na_2S. The Teflon-bonded carbon electrode used in the cathode compartment was identical to the one described before. The OCV of the cell initially was 1.38V. The cell exhibited a resistance at 130°C of 23Ω. The cell was cycled at 10 mA or about 1 mA/cm^2. The charge/discharge curves are shown in Figure 19. The first charge curve 1C, to 2.7 volt corresponds to ∿0.33 e$^-$/S. Only about 17% of Na_2S was utilized in the charging process. It appears that Na_2S was poorly distributed on the carbon electrode so that most of it was not available for the cell process. The first discharge, curve 1D, commenced at 1.6V, but in ∿20 mAh the cell polarized to ∿1.1V and further discharged proceeded at ∿1.1V. This discharge voltage is considerably lower than for the Na/DMAC/Na_2S_n cells. The second charge corresponded to ∿0.8e$^-$/S. Evidently more Na_2S was available for the charging process. The second discharge, curve 2D, proceeded with voltage fluctuations and the cell reached the 1V limit in about 4 hours or 40 mAh. The third charge, curve 3C, proceeded smoothly but at a considerably higher voltage, and after 34 mAh of charge the cell open circuited to the voltage of the current source. The experiment was terminated.
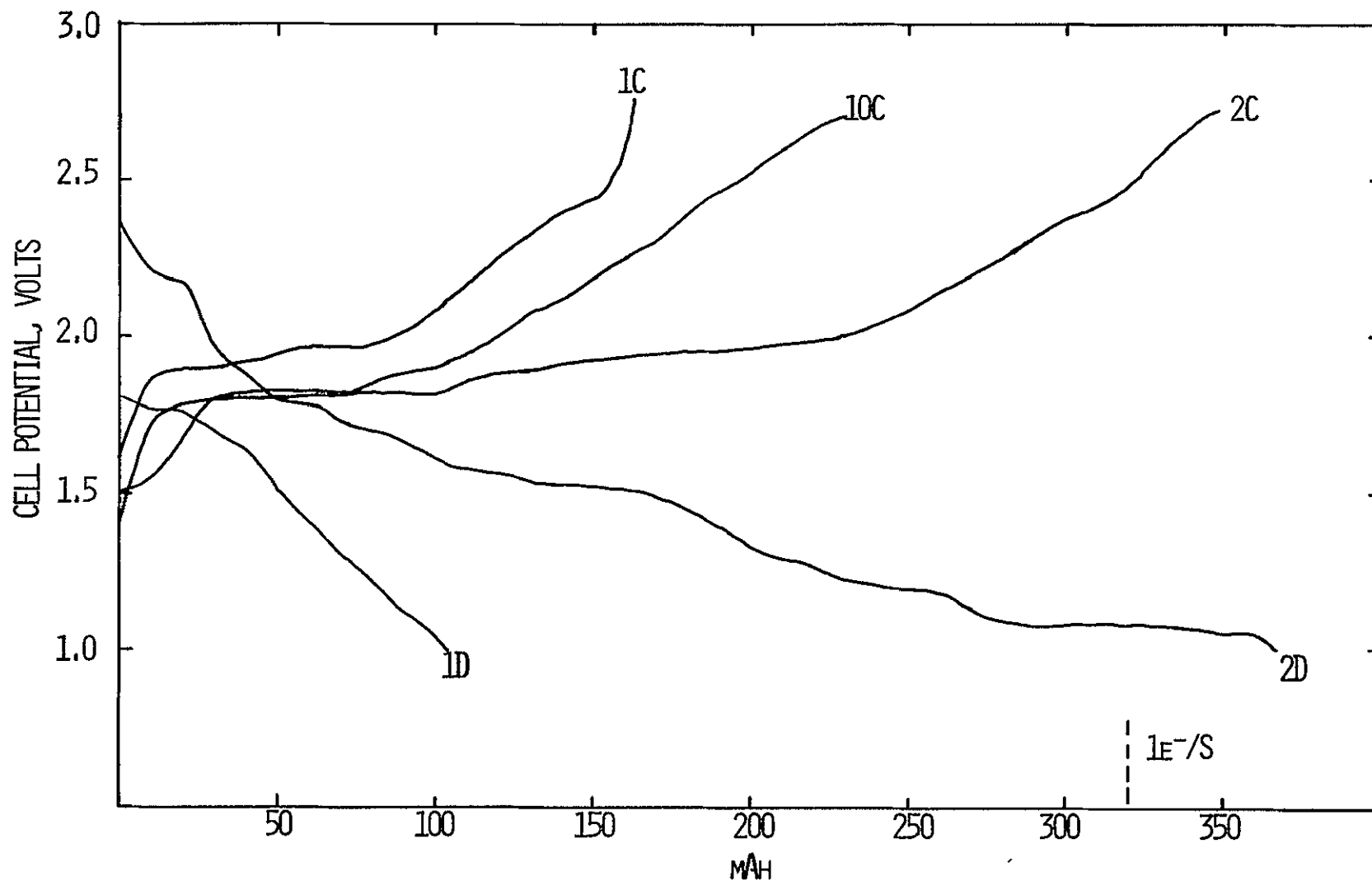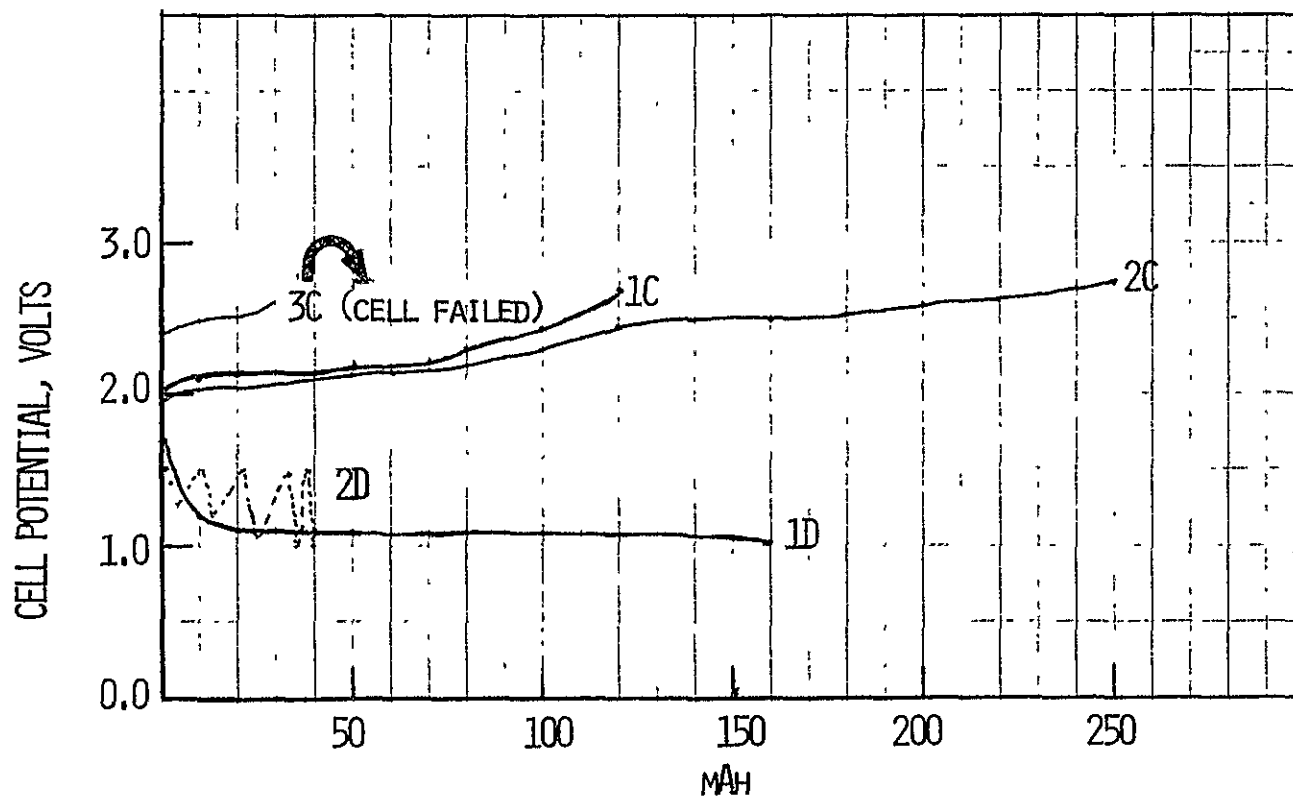
Fig. 19: Galvanostatic charge/discharge curves for a cell, liquid Na/β-Al₂O₃/ Na₂S (2M S), 0.5M NaBr, CHD/Teflon-bonded C at 130°C. Current = 10 mA. Current density = 1 mA/cm².

2. Cell with CHD/Na$_2$S$_4$/0.5M NaI Solution as the Initial Catholyte

The cell initially contained 9 ml of a 2M S solution as Na$_2$S$_4$ in CHD/0.5M NaI electrolyte. All the other features of the cells were similar to those in the cell with CHD/Na$_2$S as the initial catholyte. The OCV of the cell at 130°C was 1.83V and the cell exhibited a resistance of 25Ω. The resistance was twice that found for cells with DMAC/Na$_2$S$_n$ or DEAC/Na$_2$S$_n$ cathodes and having the same type of β-Al$_2$O$_3$ tube. The higher resistance was probably due to the higher viscosity of CHD. The galvanostatic discharge and charge curves at 9 mA or 1 mA/cm^2 are shown in Figure 20. As observed previously, the discharge begins at ∿1.6V, but the cell polarizes immediately to a plateau of 1.25V. This initial polarization to the 1.25V plateau is more pronounced in the second discharge (2D). The first discharge proceeded for 194 mAh (0.4e$^-$/S), at which point a malfunction of the cycler caused the cell to charge. The charge capacity to 2.7V was, however, much less than the previous discharge; i.e., only 110 mAh (0.23e$^-$/S). The second discharge (2D) proceeded for 650 mAh. After accounting for the charge utilization in the first cycle, a charge equivalent to 640 mAh would be required to reduce the Na$_2$S$_n$, present at the beginning of 2D to Na$_2$S. The discharge capacity of 650 mAh thus corresponds to the reaction

$$S_4^{-2} + 6e^- \rightarrow 4S^{-2} \tag{20}$$

This agreement, as well as the fact that a 1e$^-$ reduction of CHD would require 1.7 Ah charge, indicate that the solvent is not reduced at potentials above 1V. Nevertheless, the second charge (2C) proceeded for only 124 Ah (0.25e$^-$/S). The third discharge was less than the second charge, and the subsequent charge and discharge also showed the decreasing efficiency. The cell could not be operated after the fourth cycle.

The following conclusions may be drawn about the behavior of the CHD/Na$_2$S$_n$ cathode:

- Na-S cells with CHD/Na$_2$S$_n$ cathodes have relatively higher resistances, probably due to the higher viscosity of CHD.

- The operating voltage of the cell is low.

- Na$_2$S$_n$ can be reduced to Na$_2$S, but the cathode exhibits poor reversibility.
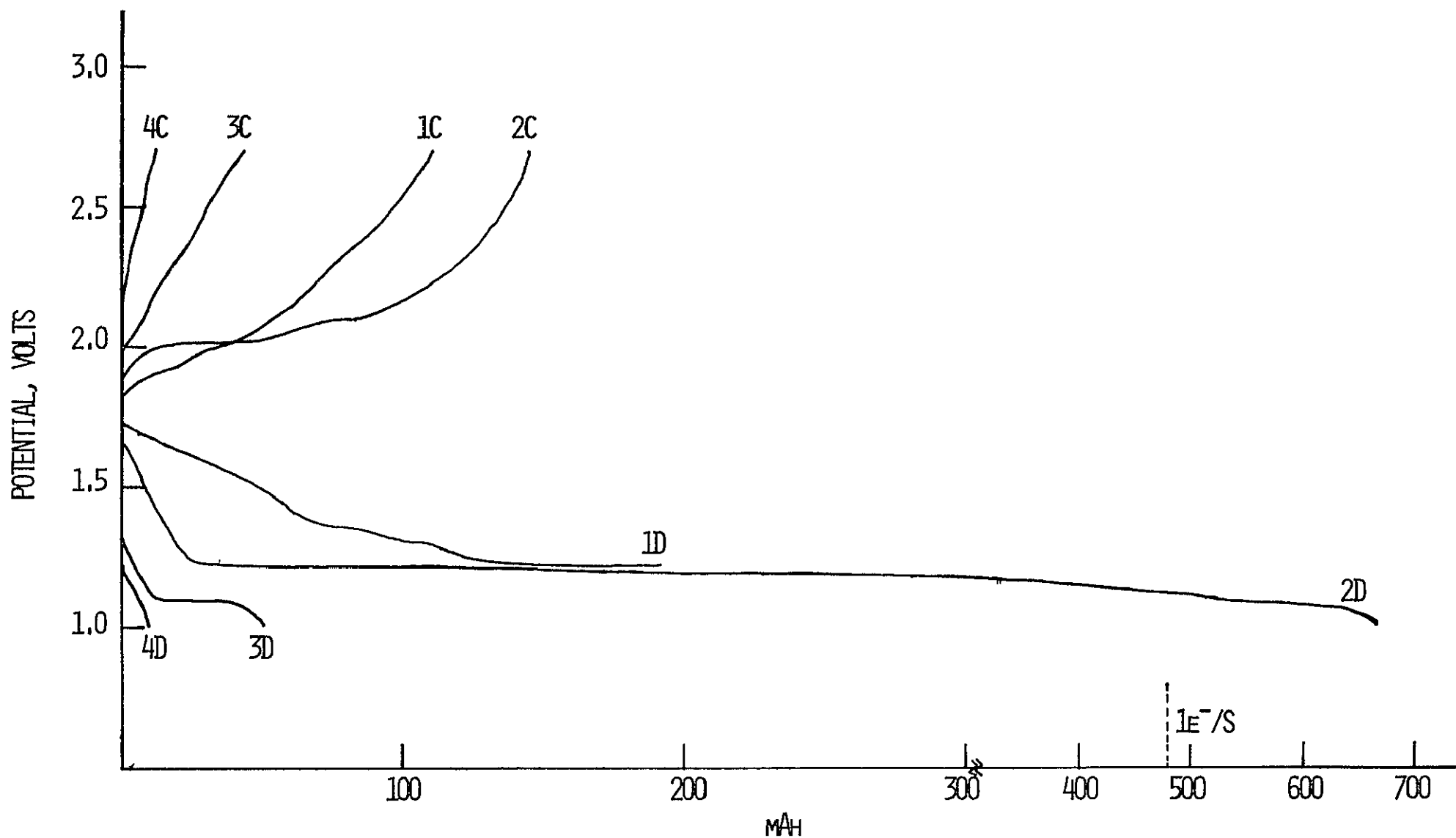
Fig. 20: Galvanostatic discharge/charge curves for the cell liquid Na/β-Al$_2$O$_3$/CHD, 0.5M NaI, 2M S as Na$_2$S$_4$ (9 ml)
Teflon-bonded C at 130°C. Current = 9 mA; current density = 1 mA/cm^2. The cell was discharged
first.

43

III. THE Na-TRANSITION METAL SULFIDE BATTERY

A preliminary evaluation of transition metal disulfides as possible cathode materials for the Na battery was done using the disulfides, TiS_2 and TaS_2. They were separately evaluated in a cell of the configuration,

$$Liquid\ Na/\beta-Al_2O_3/MS_2,\ DMAC,\ NaI$$
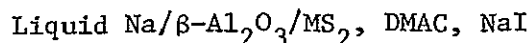
The DMAC/NaI solution served as the Na^+-ion conducting electrolyte. The experiments were conducted at 130°C.

A.   Preparation and Characterization of the Disulfides

1. Titanium Disulfide, TiS2

Titanium disulfide, TiS_2, was prepared by the direct reaction of stoichiometric amounts of Ti metal and S vapor at ∿750°C. The reaction was carried out in a sealed, evacuated (10^{-3} torr) quartz tube under a temperature gradient achieved in a tube furnace.

In a preparation, 7g Ti metal powder (100 mesh) and 9.6g S (Ventron, crystals, 99.99%) were introduced into either end of a thick-walled quartz tube of 25 mm OD and 57 cm long. The tube was evacuated (10^{-3} torr) and sealed off. It was then introduced into a three-zoned furnace and heated with the temperature profile shown in Table 7. After heating, the tube was allowed to cool to room temperature and the TiS_2 was collected. It was a dark green solid with a distinct yellow metallic luster when spread into the form of a thin film. The X-ray diffraction pattern for a sample of TiS_2 prepared by the same procedure as is shown in Table 8. The experimental values are in good agreement with those calculated for hexagonal TiS_2.

The titanium content of the sulfide was analyzed as the oxide, according to the reaction

$$TiS_2 + 3O_2 \xrightarrow{\ 700°C\ } TiO_2 + 2SO_2 \qquad (21)$$
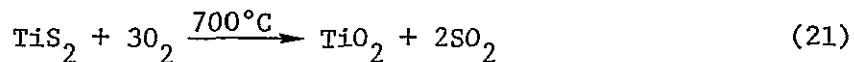
In this procedure, 0.5235g of TiS_2, contained in a preweighed alumina crucible, was ignited in air at 700°C until all the sulfide was converted to the oxide. The oxide weighed 0.3785g which was equivalent to 43.4% Ti in the disulfide sample. The formula of the disulfide was calculated to be $Ti_{1.02}S_2$.

TABLE 7

TEMPERATURE PROFILE FOR THE PREPARATION
OF TiS$_2$ FROM Ti and S

Time (hr) at Each Temp.	Temperature, °C		
	Zone A (15 cm long) (Titanium Metal)	Zone B (30 cm long)	Zone C (15 cm long) (Sulfur)
1	500	500	400
2.5	550	550	400
19	600	600	400
29	650	650	400
20	700	700	400
27	750	750	600

TABLE 8

X-RAY DIFFRACTION DATA CALCULATED FOR HEXAGONAL TiS_2
AND OBSERVED LINES OF SAMPLES PREPARED BY
THE PRESENT PROCEDURE

Calculated		Experimental	
$2\theta<$	Intensity	$2\theta<$	Intensity
15.6	500	not done	
34.2	1000	34.4	1000
–	–	39.8	149
44.1	450	44.4	505
–	–	48.0	75
53.9	250	54.0	333
56.4	80	56.6	118
57.5	160	57.9	204
65.3	100	65.4	268
72.1	80	72.3	129
–	–	75.0	53
89.5	80	89.8	225
89.7	100	–	–

2. Tantalum Disulfide, TaS_2

The tantalum disulfide was purchased from Cerac Inc., Milwaukee, Wisconsin (Catalog No. T-1018). Its X-ray diffraction data, according to the manufacture, matched the pattern* for hexagonal TaS_2. We analyzed the Ta content of the disulfide as the oxide, Ta_2O_5, using the reaction

$$2TaS_2 + 6\tfrac{1}{2}O_2 \xrightarrow{\text{700°C}} Ta_2O_5 + 4SO_2 \qquad (22)$$
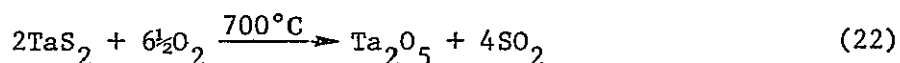
In the analysis, 0.6051g TaS_2 gave 0.5482g Ta_2O_5, which corresponded to 74.2% Ta in the disulfide sample. The formula of the disulfide was calculated to be $Ta_{1.01}S_2$.

B. Stability Characteristics of Metal Sulfide/Amide Mixtures

The long term stability characteristics of dimethylacetamide (DMAC), diethylacetamide (DEAC) or their NaI solutions in the presence of TiS_2 at 130°C were evaluated by the sealed tube technique. Titanium disulfide was insoluble in these amides both at room temperature and at 130°C. The tests were performed with mixtures of the amide or its NaI solution containing an excess of undissolved TiS_2. The various test mixtures and the results are shown in Table 9. No gases were produced from any of these mixtures even after 43 days of heating at 130°C. After the heating, the liquid was analyzed by UV-visible and infrared spectroscopy. The liquid from each of the test mixtures exhibited a weak but broad absorption beginning at ∿500 nm and tailing off into the UV. This absorption pattern resembled that of the reaction products of S with the amides, described earlier and it might be due to minor products resulting from the reaction of unreacted S in the TiS_2 with the amides.

The results seemed to indicate that the overall stability of the amides in the presence of the disulfides was acceptable. However, it should be noted that since the amides are basic solvents, their intercalation with the metal chalcogenide is possible. This was not investigated.

C. Electrochemical Evaluation of Transition Metal Disulfides

1. Titanium Disulfide as the Cathode

● Preparation of Pressed Electrodes

A mixture of TiS_2 and Teflon powder (90:10 w/o) was intimately mixed with a mortar and pestle for ∿20 minutes. The cathode mix was bonded

---

*See Powder Diffraction File, No. 2-0137.

TABLE 9

STABILITY TEST DATA FOR AMIDE/TiS$_2$ MIXTURES AT 130°C

Tube No.	Reactants	No. of Days at 130°C	mmoles of Gas	Comments
A	0.47g TiS$_2$, 2 ml DMAC	43	no gas	light brown liquid over dark grey powder
B	0.49g TiS$_2$, 0.31g NaI, 2 ml DMAC	43	no gas	light green liquid over dark grey powder
C	0.49g TiS$_2$, 2 ml DEAC	43	no gas	orange-red liquid over dark grey powder
D	0.46g TiS$_2$, 0.31g NaI, 2 ml DEAC	43	no gas	orange-red liquid over dark grey powder

to an expanded nickel screen by pressing at $\sim$4800 psi for $\sim$10 minutes at
a temperature of 250°C. The pressed electrode had an average thickness
of 0.56 mm. The electrode was weighed to determine the TiS_2 content
before incorporating in the electrochemical cell.

◉ Cell Studies

The cell setup was done as described previously for the soluble
S cathode with a liquid $Na/\beta-Al_2O_3$ counter electrode. The TiS_2 cathode
measured 6.5 cm × 2.5 cm and contained 1.42g TiS_2. A solution of 1M NaI
in DMAC formed the catholyte. The cell, at 130°C, exhibited an unusually
high impedance of $\sim$60Ω. The discharge was performed at 4 mA (0.2 mA/cm^2).
The discharge and charge are shown in Figure 21. The initial OCV was 2.19V.
Three plateaus are evident in the discharge curve for the sodium contents,
x, of $0.41 < x$, $0.41 < x < 0.66$ and $0.68 < x \leq 0.95$. These values are based on the
weighed amount of TiS_2 originally present in the cell; 1.42g or 340 mAh.

A previous electrochemical cell study (19) also showed three plateaus
for the discharge, but at slightly different ranges of the Na content, i.e.,
$0.45 < x$, $0.45 < x < 0.80$ and $0.80 < x \leq 1$. However, these were found to be dependent
on the composition of the sulfide, i.e., on x in $Ti_{1+x}S_2$. Also, these values
were obtained at room temperature and the electrolyte was propylene carbonate/
NaI.

Our data show that the three phases are formed at the higher tempera-
ture also. The different ranges of x values for the three phases in the
present study may have resulted from the higher temperature condition or
from the different solvent employed here.

The charge curve also showed three regions at essentially the same
ranges of Na contents. The rechargeability of the cathode was sluggish at
higher rates. In one experiment, it was possible to cycle the cathode
several times, Figure 22, at reasonably high discharge rates, but keeping
charges at low current densities. It can be seen that the efficiency after
the first cycle remained essentially constant. In general it was found
difficult to charge compositions of Na_xTiS_2 with $x \leq 0.4$. The exact reasons
for this were not investigated. Factors such as co-intercalation of the
solvent and phase transitions in the ternary system, Na_xTiS_2, are possible
reasons.

2. Tantalum Disulfide as a Cathode

◉ Preparation of Pressed Electrodes

An electrode was prepared by a slightly modified procedure used
for the TiS_2 electrodes. An intimate mixture of the disulfide and Teflon
powder (92:8 w/o) was cold-pressed onto an expanded nickel screen (Exmet

49
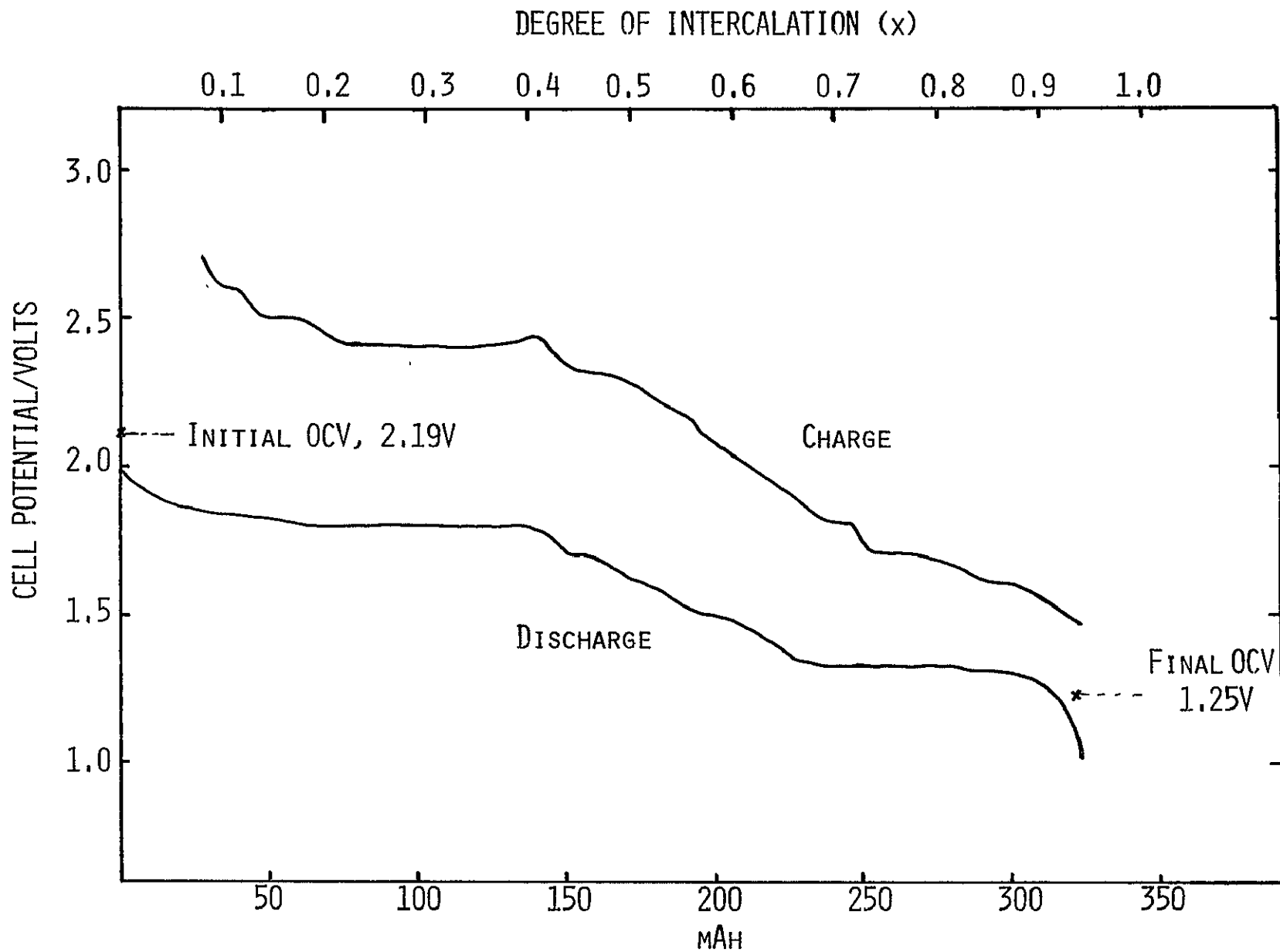
Fig. 21: The discharge/charge curves for the cell liquid Na/β-Al$_2$O$_3$/DMAC (1M NaI), TiS$_2$ at 130°C. Current = 4 mA, current density = 0.2 mA/cm^2.

DEGREE OF INTERCALATION (X)
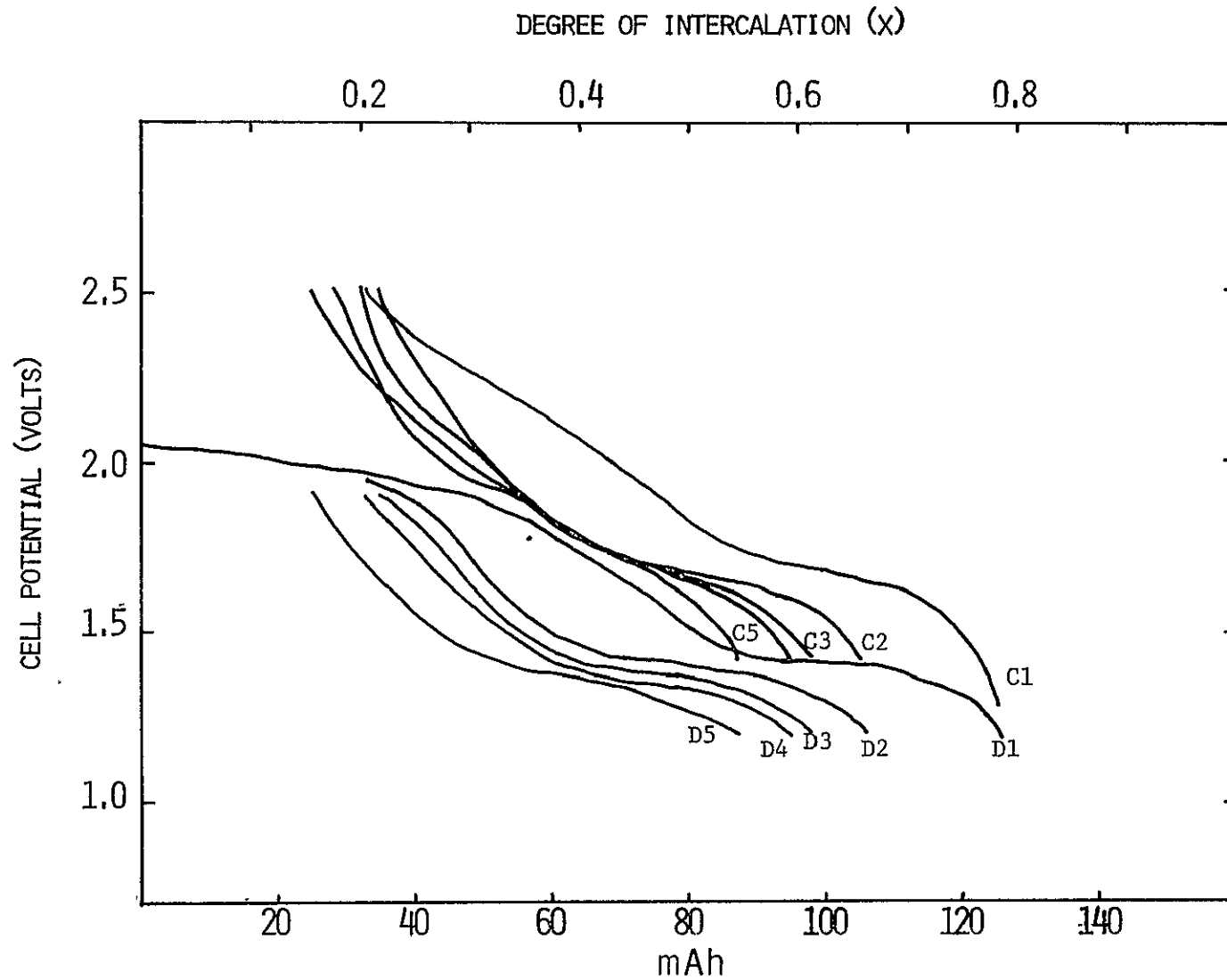
Fig. 22: Galvanostatic discharge/charge curves for the cell liquid Na/β-Al₂O₃/DMAC (1M NaI), TiS₂ at 130°C. Dl thru D-5 are discharge curves. Current = 20 mA (∿4 mA/cm² of β-Al₂O₃). Cl thru C5 are charge curves. Current = 5 mA or (∿1 mA/cm² of β-Al₂O₃).

Corp. 5 Ni 5 - 5/0) at 5600 psi for ∿6 minutes. The pressed electrode was then sintered in an argon atmosphere at 300°C for half an hour. We also prepared electrodes with NaTaS$_2$. In this case, the cathode was cold-pressed but no sintering was done afterwards.

● Cell Studies

Two kinds of experiments were carried out: (i) initial discharge and subsequent cycling of the fully charged cathode, TaS$_2$; (ii) initial charge and subsequent cycling of the fully discharged cathode, NaTaS$_2$. The NaTaS$_2$ was prepared chemically from Na naphthalide and TaS$_2$ in tetrahydrofuran as described later.

Tests with the TaS$_2$ Cathode. The cell utilized 1M NaI/ DMAC electrolyte. A plot of the discharge potential (volts) vs. the degree of Na intercalation (mole Na/mole TaS$_2$) is shown in Figure 23 (curve A). The cell EMFs corresponding to the various degrees of Na intercalation are shown in curve B, Figure 23. Both of these curves show fairly linear transitions to lower potentials as the amount of intercalated Na is increased from zero to one. At a discharge cutoff voltage of 1.00V, only 0.8 mole of Na per mole of TaS$_2$ was intercalated. The EMF corresponding to this composition was 1.20V. The EMF value corresponding to the fully intercalated compound, NaTaS$_2$ was obtained from a cell incorporated with this material initially as the cathode. The EMF was 0.97V at 130°C. It thus appears that in order to achieve full intercalation of the TaS$_2$ lattice, the lower limit of the operating cell voltage has to be below 1.00V when the electrolyte is DMAC/NaI. The EMF-composition curve for the Na$_x$TaS$_2$ ternary system for values of x from zero to one in DMAC/NaI at 130°C, constructed from the two sets of data, is shown in Figure 23 (curve B).

The EMF-composition curve for the Na$_x$TaS$_2$ system is different from that observed with the Na$_x$TiS$_2$ ternary. The present data for Na$_x$TaS$_2$ are in agreement with a previous study (20) on TaS$_2$ at room temperature using PC/NaI electrolyte (see also inset in Figure 23). In that study, the EMF-composition data along with the X-ray results indicated a single phase ternary system for Na$_x$TaS$_2$ for all values of x, 0<x<1. The present data suggest the formation of a single phase ternary system also in the DMAC/NaI electrolyte at 130°C. The EMF-composition curve does show some deviations from linearity at low and high x values. This, in the absence of X-ray data, may be attributed to the different solvent employed here. The experimental data in the previous study also showed this behavior at low x values, but X-ray revealed only one phase.

Tests with NaTaS$_2$ Cathode. The fully Na intercalated disulfide, was prepared according to the reactions,

DEGREE OF INTERCALATION (X)

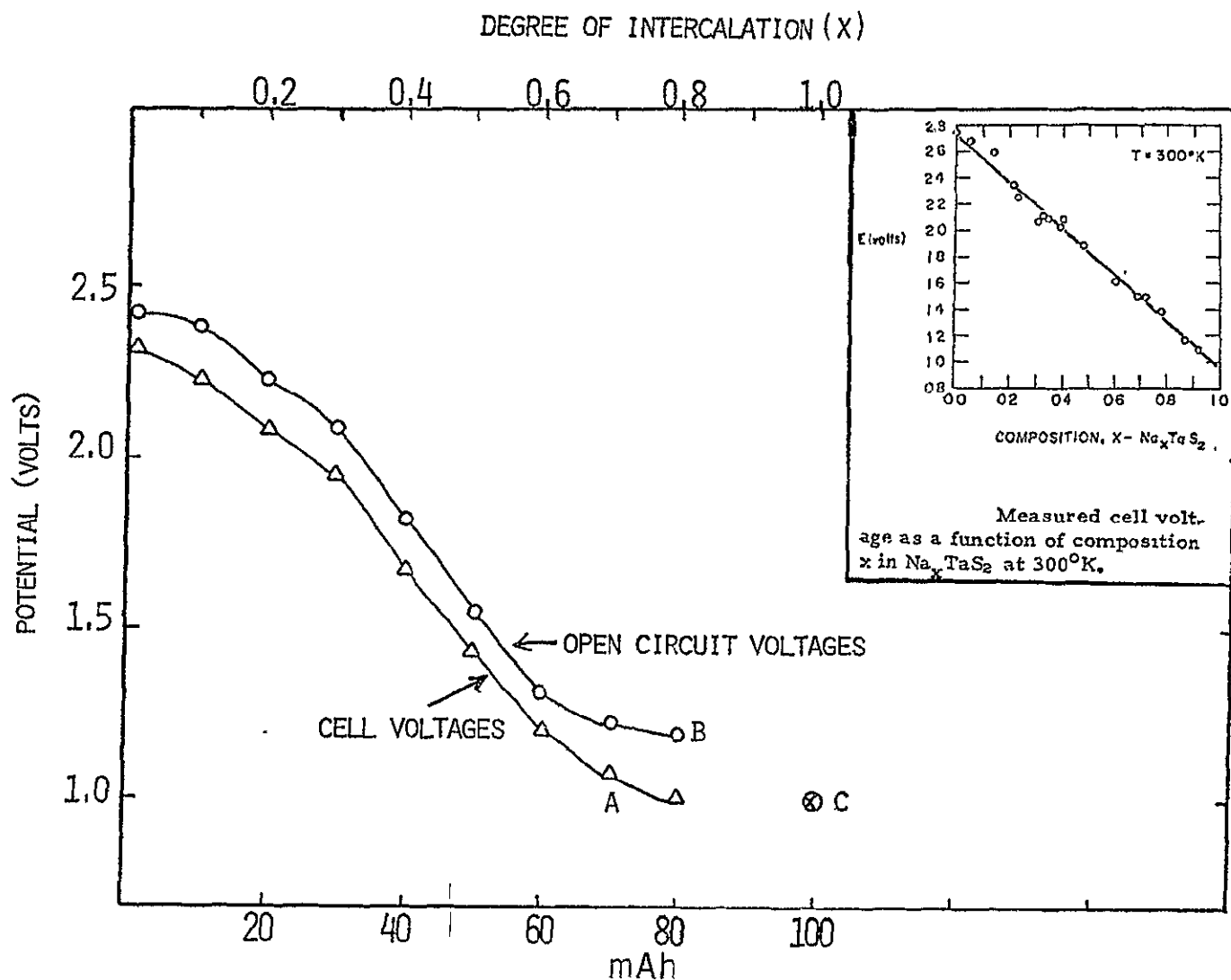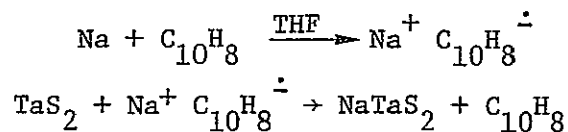Fig. 23: The galvanostatic discharge curve for the cell liquid Na/β-Al₂O₃/DMAC (1M NaI), TaS₂ at 130°C. Curve A is the plot of cell potential vs. degree of Na intercalation. Curve B is the plot of open-circuit voltage of the cell as a function of Na intercalation. C is the open-circuit voltage obtained with NaTaS₂ as the cathode. Current = 10 mA or ~2.0 mA/cm² of β-Al₂O₃. Inset is the data from Ref. 3.

$$Na + C_{10}H_8 \xrightarrow{THF} Na^+ \, C_{10}H_8^{\cdot -}$$

$$TaS_2 + Na^+ \, C_{10}H_8^{\cdot -} \rightarrow NaTaS_2 + C_{10}H_8$$

In a preparation, 2.61g (20.4 mmoles) of naphthalene and 0.47g (20.4 mmoles) of Na were mixed in ~50 ml THF and stirred overnight at room temperature to obtain a dark green solution of the naphthalide anion radical. The exact Na concentration of the solution was analyzed by treating an aliquot of the solution (2 ml) with an excess of standard HCl and then back-titrating the unreacted HCl with a standard solution of NaOH using phenolphthalein as the indicator. To 48 ml of the naphthalide solution, 4g (16.3 mmoles) of TaS_2 were added, and the mixture was stirred for 2 days. The Na_xTaS_2 product was filtered, washed with THF and finally dried in vacuum. The Na_xTaS_2 product was collected as a very shiny dark grey material. The filtrate was analyzed for its Na content. The composition of the intercalated material was calculated to be $Na_{1.05}TaS_2$. The EMF value of 0.97V vs Na^+/Na for this material also suggests a composition with x very close to one. This material was used for testing the rechargeability of the TaS_2 cathode.

Rechargeability of TaS_2 Cathode. The rechargeability of the cathode in DMAC/NaI electrolyte appeared to be kinetically limited as evidenced by data from cells in which the cathode initially was either TaS_2 or Na_xTaS_2. In general, the efficiency of rechargeability increased with decreasing current density. It was also found that the EMF-composition curve during charge showed considerable deviation from that during discharge for the same degree of Na intercalation, Figure 24. The galvanostatic charge curves, obtained from the two different initial cathode compositions, however, showed analogous voltage-composition behavior.

The work carried out herein suggests that transition metal disulfides present good possibilities as cathode materials in moderate temperature Na batteries. Further work should concentrate on a search for suitable electrolytes that can accommodate high rate battery operation and on selection of cathode materials with minimum phase transition. A most important issue is the inter-relationship between phase changes during Na intercalation and the rechargeability of the cathode. This needs to be systematically explored.
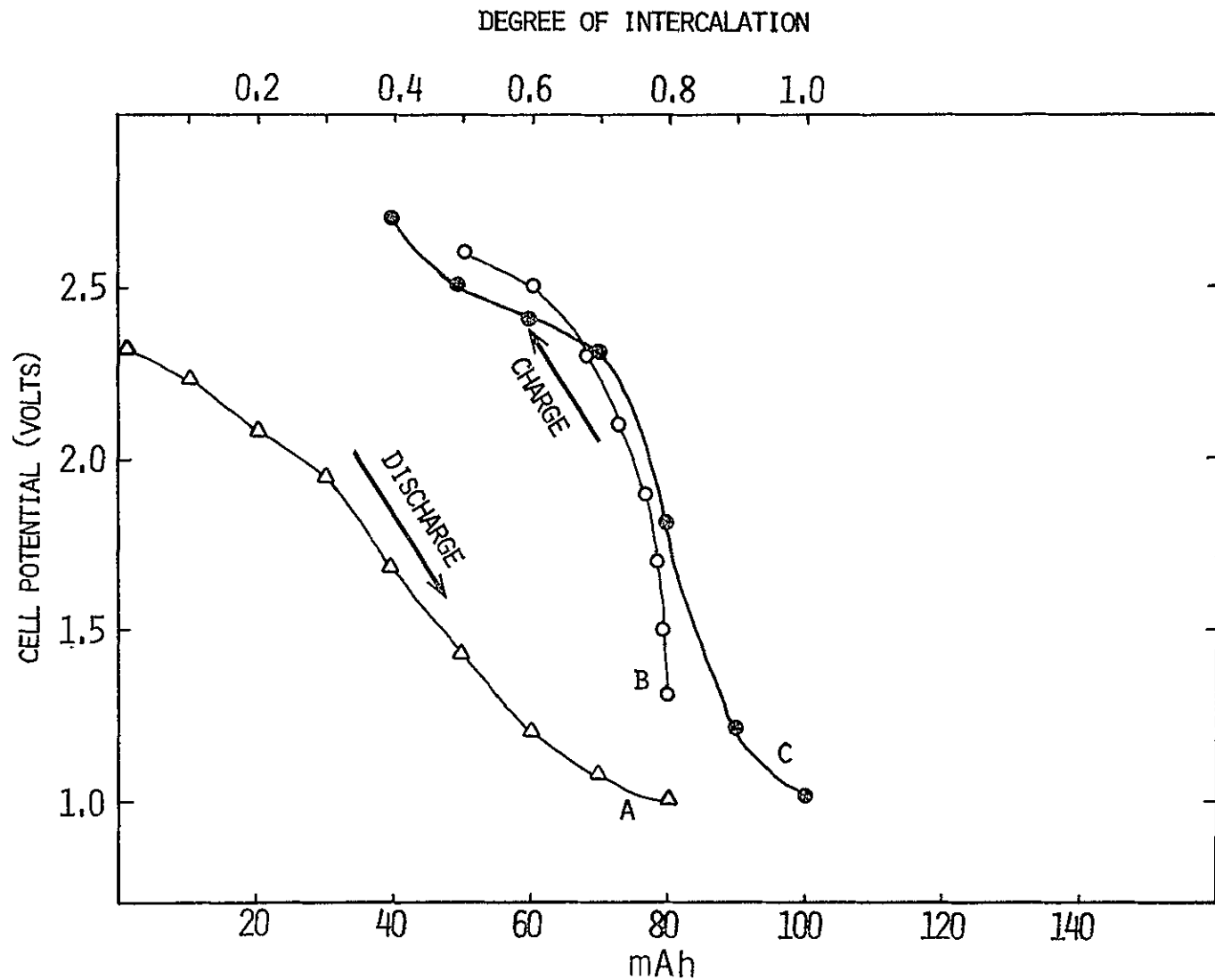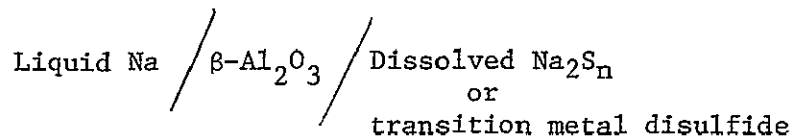
DEGREE OF INTERCALATION

Fig. 24: Galvanostatic discharge/charge curves A and B for the cell liquid Na/β-Al₂O₃/ DMAC (1M NaI), TaS₂ at 130°C. Current = 10 mA (∿2 mA/cm² of β-Al₂O₃). Curve C is the charge curve for a cell with NaTaS₂ initially in the cathode, current = 5 mA (∿1.0 mA/cm² of β-Al₂O₃).

IV. SUMMARY AND CONCLUSIONS

The feasibility of a moderate temperature Na battery having the configuration

$$\text{Liquid Na} \bigg/ \beta\text{-Al}_2\text{O}_3 \bigg/ \begin{array}{c} \text{Dissolved Na}_2\text{S}_n \\ \text{or} \\ \text{transition metal disulfide} \end{array}$$

has been investigated. The operating temperature of the battery is 130°C. Two kinds of cathode were investigated (i) a soluble S cathode consisting of a solution of Na_2S_n in an organic solvent and (ii) an insoluble S cathode consisting of a transition metal dichalcogenide in contact with a Na^+-ion-conducting electrolyte.

A series of aliphatic amides was investigated in an attempt to find a suitable solvent for the soluble S cathode with special emphasis on long term stabilities in the presence of Na_2S_n. The dialkyl substituted amides were found to be the most stable. They did show some reactivity during long term heating with Na_2S_n, $n > 4$. However, isolation studies indicated that the reactive species in these solutions was the elemental sulfur present in equilibrium. The stability studies also indicated that relatively longer cycle life could be obtained for the CH_3CONR_2/Na_2S_n cathode if the cell operation is limited to the cycling regime.

$$S_4^{-2} + 6e^- \rightleftarrows 4S^{-2}; \ 1.5e^-/S$$
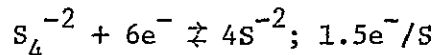
Cell cycling studies using the solutions $CH_3CON(CH_3)_2/Na_2S_n$ or $CH_3CON(C_2H_5)_2/Na_2S_n$ indicated that these cathodes were reversible and that the reduction of S_n^{-2} to S^{-2} could be achieved with a highly porous cathode current collector structure.

The suitability of 1,3-cyclohexanediol as a solvent for the soluble S cathode was also investigated. It was found that this solvent is stable with respect to Na_2S_n for long periods of time and that it dissolves moderate amounts of Na_2S. However, the electrochemical reversibility of 1,3-cyclohexanediol/Na_2S_n solutions was poor.

A limited amount of study was carried out to determine the suitability of transition metal dichalcogenides as possible cathodes for the Na battery. Our results of studies with TaS_2 or TiS_2 indicated that the phase transitions during intercalation of Na into the transition metal dichalcogenides are strongly dependent on the structure of the dichalcogenide themselves. In general, transition metal disulfides present good possibilities as cathode materials for the moderate temperature Na battery.

56

V. REFERENCES

1. Annual Report on the Ford Sodium-Sulfur Battery, Contract NSF-C805 (AER73-07199), July 1976.

2. C. Levine, Proc. 10th IECEC Meeting, p. 621 (1975).

3. J. T. Kummer and N. Weber, Auto. Eng. Cong., Detroit, Michigan, S.A.E. 670179 (1967).

4. N. K. Gupta and R. P. Tischer, J. Electrochem. Soc. 119, 1003 (1972).

5. Y. K. Kas and P. C. Wagner, J. Electrochem. Soc. 123, 623 (1976).

6. G. L. Holleck and J. R. Driscoll, Electrochim. Acta. 22, 647 (1977).

7. S. P. Mitoff and J. B. Bush, Jr., Proc. 9th IECEC Meeting, p.916 (1974).

8. J. Werth et al., ESB Inc., Report on EPRI Research Project 109-2-1, June 1975.

9. J. Werth, paper presented at Argonne National Laboratory Workshop on High Temperature Batteries, March 1976.

10. K. M. Abraham, R. D. Rauh and S. B. Brummer, Electrochim. Acta, 23, 501 (1978).

11. D. F. Shriver, The Manipulation of Air Sensitive Compounds (New York: McGraw-Hill, 1969).

12. J. A. Riddick and W. B. Bunngen in Organic Solvents (New York: Wiley-Interscience, 1970).

13. D. S. Reid and C. A. Vincent, J. Electroanal. Chem. 18, 427 (1968).

14. W. Blaedel and V. Meloche, Elementary Quantitative Analysis, 2nd ed. (Harper and Row, 1963), p.463.

15. R. Fritz and P. Yamamura, Anal. Chem. 27, 9 (1955).

16. B. Lux et al., Chem. Bev., 101, 2485 (1968).

17. S. B. Brummer, et al., "Low Temperature Lithium/Sulfur Secondary Battery," Annual Progress Report, ERDA Contract No. EY-76-C-02-2520, June 1977.

18. D. R. Cogley and M. J. Turchan, First Quarterly Report on Contract DAAB07-74-C-0030, December 1973.

19. D. A. Winn et al., Mat. Res. Bull., 11, 449 (1976).

20. A. S. Nagelberg and W. L. Worrell, Proceedings of the Symposium on Electrode Materials and Processes for Energy Conversion and Storage, The Electrochemical Society, p.487 (1977).

DISTRIBUTION LIST

Dr. Ted Beck
Electrochemical Technology Corp.
3935 Leary NW
Seattle, WA   98107

Dr. Douglas Bennion
Energy and Kinetics Department
School of Engineering & Applied Science
University of California
Los Angeles, CA   90024

Mr. William Botts
Program Manager
Atomics International
P.O. Box 309
Canoga Park, CA   91304

Mr. John Bush
General Electric Corp.
Research and Development Center
P.O. Box 8
Schenectady, NY   12301

Dr. Alina Boruka
Boruka Research Co.
60 Chestnut Street
Livingston, NJ   07039

Dr. Jack Brown
Research Laboratory
Westinghouse Electric Corp.
1310 Beulah Road
Pittsburgh, PA   15235

Dr. Ralph Brodd
Research Laboratories
Union Carbide Corp.
Parma, OH   44129

Mr. Earl Carr
Eagle Picher Industries, Inc.
Electronics Div., Couples Dept.
P.O. Box 47
Joplin, MO   64801

Dr. David Douglas
Vice Pres., Contract Research
Gould, Inc.
40 Gould Center
Rolling Meadows, IL   60008

Dr. Morris Eisenberg
Electrochimica Corp.
2485 Charleston Road
Mountain View, CA   94040

Dr. D. Thomas Ferrell
ESB Technology Center
19 West College Avenue
Yardley, PA   19067

Dr. A. Donald Galbraith
Power Cell Program Office
Lockheed Palo Alto Research Lab
3251 Hanover Street
Palo Alto, CA   94304

Dr. Jose Giner
Giner, Inc.
144 Moody Street
Waltham, MA   02154

Dr. Gilbert Goodman
Globe-Union, Inc.
Milwaukee, WI   53201

Dr. Robert Huggins
Stanford University
Center for Materials Studies
Stanford, CA   94305

Mr. Henry Jensen, V.P.
C&D Batteries
3042 Walton Road
Plymouth Meeting, PA   19462

Dr. Charles A. Levine
Dow Chemical Research Labs
Walnut Creek Center
2800 Mitchell Drive
Walnut Creek, CA   94598

Prof. Prem Mahendroo
Department of Physics
Texas Christian University
Fort Worth, TX   76129

Dr. John Newman/Dr. Charles Tobias
Department of Chemical Engineering
University of California
Berkeley, CA   94720

Dr. A. Skopp, Director
Advanced Energy System Laboratory
Exxon Research & Engineering Company
P.O. Box 8
Linden, NJ   07036

Dr. Robert Selman
Illinois Institute of Technology
3300 South Federal
Chicago, IL   60616

Dr. S. Weiner
Ford Corp.
Chemical Engineering Department
Scientific Research Staff
20000 Rotunda Drive
Dearborn, MI   48121

Mr. Ralph Zito
GEL, Inc.
1511 Peace Street
Durham, NC   27701

Catalyst Research Corp.
1421 Clarkeview Road
Baltimore, MD   21209

Yardney Electric Corp.
82 Mechanic Street
Pawcatuck, CT   02891

Energy Research Corporation
3 Great Pasture Road
Danbury, CT   06810

Dr. Ernest Yeager
Case-Western Reserve University
Electrochemistry Research Lab
Cleveland, OH   44106

Giovanni Caprioglio
General Atomic Co.
P.O. Box 81608
San Diego, CA   93128

Commander, Naval Sea Systems Command
Department of the Navy
Arlington, VA   20362

Defense Documentation Center
Cameron Station - Bldg. 5
Alexandria, VA   22314

National Aeronautics & Space Admin.
Washington, D.C.   20546
Attn: RPP

Command Officer
US Army Electronics R&D Labs
Fort Monmouth, NJ   07703
Attn: Mr. David Linden (DRSEL-TL-P)

Frank J. Seiler Research Lab (AFSCO)
FJSRL-WC
USAF Academy, CO   80840
Attn: Capt. Erbacher

Harry Diamond Laboratories
Chief, Power Supply Branch
2800 Powder Mill Road
Adelphi, MD   20783
Attn: Mr. A. A. Benerley

Flight Vehicle Power Branch
Air Force Aero Propulsion Lab
Wright-Patterson AFB, OH   45433

Institute for Defense Analysis
R&E Support Division
400 Army-Navy Drive
Arlington, VA   22202
Attn: Mr. R. Hamilton

Office of Naval Research (Code 472)
800 North Quincy Street
Arlington, VA   22217
Attn: Dr. George A. Neece

Naval Ship Engineering Center
Center Building
Prince Georges Center
Hyattsville, MD   20783
Attn: Mr. A. Himy, Code 6157D

NASA Scientific & Technical (30 copies)
  Information Facility
Baltimore/Washington Intl. Airport
P.O. Box 8757
.Maryland   21240

Institute of Gas Technology
3424 S. State Street
IIT Center
Chicago, IL   60616
Attn: K. Blurton

Dr. Arthur Fleischer
466 South Center Street
Orange, NJ   07050

Furukawa Battery Co., Ltd.
No. 246, Z-Chome
Hoshikawa-Cho
Hodogaya, Yokohama, Japan
Attn: K. Shimizu

Gates Energy Products, Inc.
999 S. Broadway
Denver, CO   80217
Attn: E. Seo

General Dynamics
Convair Aerospace Division
Dept. 623-2
P.O. Box 80847
San Diego, CA   92138
Attn: R. P. Mikkelson

Battery Business Dept.
General Electric Company
P.O. Box 114
Gainesville, FL   32602
Attn: M. Kronenberg

General Electric Company
Space Systems
Room M-2700, P.O. Box 8555
Philadelphia, PA   19101
Attn: K. L. Hanson

General Electric Company
777 14th Street, NW
Washington, DC   20005
Attn: D. F. Schmidt

General Motors Research Labs
Electrochemistry Department
Warren, MI   48090
Attn: R. G. Gunther

General Motors Research Labs
Electrochemistry Department
Warren, MI   48090
Attn: E. J. Cairns

Globe-Union, Inc.
Corporate Applied Research
5757 North Green Bay Avenue
Milwaukee, WI   53201
Attn: W. L. Towle

Grumman Aerospace Corp.
OAO Project
Plant 35
Bethpage, Long Island, NY   11714
Attn: S. J. Gaston

G&W H. Corson, Inc.
Plymouth Meeting, PA   19462
Attn: L. J. Minnick

Chrysler Corp.
Space Division
Department 2730
P.O. Box 29200
New Orleans, LA   70189
Attn: C. E. Thomas

Communications Satellite Corporation
Comsat Laboratories
P.O. Box 115
Clarksburg, MD   20734
Attn: R. Strauss

Delco Remy Division
General Motors Corp.
2401 Columbus Avenue
Anderson, IN   46011
Attn: J. A. Keralla

E. I. DuPont de Nemours & Co.
Engineering Materials Lab
Building 304
Wilmington, DE   19898
Attn: J. M. Williams

Dynatech Corp.
17 Tudor Street
Cambridge, MA   02139
Attn: R. L. Wentworth

Exxon Research & Engineering Company
Government Research Lab
P.O. Box 8
Linden, NJ   07036
Attn: L. Berkowitz

ESB, Inc.
Box 6266
Cleveland, OH   44101
Attn: G. Hobbib

EST, Inc.
Ray-O-Vac
630 Forward Drive
Madison, WI   73611
Attn: R. J. Dawson, Project Mgr.

Electrochemical & Water Desal.
  Technology
13401 Kootenay Drive
Santa Ana, CA   92705
Attn: C. Berger

Gulton Battery Corp.
212 Durham Avenue
Metuchen, NJ   08840
Attn: E. Kantner

Hughes Aircraft Corp.
Centinda Avenue & Teale Street
Culver City, CA   90230
Attn: T. V. Carvey

Hughes Research Labs
3011 Malibu Canyon Road
Malibu, CA   90265
Attn: H. Sup Lim

Institute for Defense Analyses
400 Army-Navy Drive
Arlington, VA   22202
Attn: R. Hamilton

International Nickel Co.
1000 16th Street, NW
Washington, DC   20036
Attn: J. R. Hunt

Invention Talents, Inc.
1149 Chesapeake Avenue
Columbus, OH   43212
Attn: J. McCallum

Johns Hopkins University
8621 Georgia Avenue
Silver Springs, MD   20910
Attn: R. E. Evans

Midwest Research Institute
425 Volker Boulevard
Kansas City, MO   64110
Attn: Physical Science Lab

Johns-Manville R&D Center
P.O. Box 159
Manville, NJ   08835
Attn: J. S. Parkinson

Kimberly-Clark Corp.
New Market Development Mgr.
Neenah, WI   54956
Attn: R. T. Carpenter

Leesona Moos Laboratories
333 Strawberry Field Road
Warwick, RI   02887
Attn: A. Moos

Mallory Battery Co.
So. Broadway & Sunnyside Lane
Tarrytown, NY   10591
Attn: S. J. Angelovich

P. R. Mallory & Co., Inc.
Northwest Industrial Park
Burlington, MA   01803
Attn: P. Bro

Martin Marietta Corp.
Electronics Research Dept.
P.O. Box 179
Denver, CO   80201

McDonnell Douglas Astro. Co.
5301 Bolsa Avenue
Huntington Beach, CA   92647
Attn: Library

McGraw Edison Co.
Edison Battery Division
P.O. Box 28
Bloomfield, NJ   07003
Attn: R. C. Chudacek

Melpar-Technical Information Center
7700 Arlington Blvd.
Falls Church, VA   22046

Texas Instruments, Inc.
34 Forrest Street
Attleboro, MA   02703
Attn: J. W. Ross

Monsanto Research Corp.
1515 Nicholas Road
Dayton, OH   45407
Attn: I. O. Salyer

North American Aviation, Inc.
12214 Lakewood Blvd.
Downey, CA   90241
Attn: B. M. Otzinger

North American Rockwell
Autonetics Division
P.O. Box 4192
Anaheim, CA   92803
Attn: R. F. Fogle (GA28)

North American Rockwell Corp.
Rocketdyne Division
6633 Canoga Avenue
Canoga Park, CA   91304
Attn: Library

Philco-Ford Corp.
3939 Fabian Way
Palo Alto, CA   94303
Attn: D. C. Briggs

Power Information Center
University City Science Center
3624 Science Center
Philadelphia, PA   19104

Rensselaer Polytechnic Institute
Department of Chemistry
Troy, NY   12180
Attn: G. J. Janz

Southwest Research Institute
P.O. Drawer 28510
San Antonio, TX   78228
Attn: Library

Stanford Research Institute
333 Ravenswood Avenue
Menlo Park, CA   94025
Attn: Librarian

Texas Instruments, Inc.
P.O. Box 5936
Dallas, TX   75222
Attn: I. Trachtenberg

TRW Systems, Inc.
One Space Park (R-1/2094)
Redondo Beach, CA   90278
Attn: H. P. Silverman

Union Carbide Corp.
Parma Laboratory
P.O. Box 6116
Parma, OH   44130
Attn: Library

University of Maryland
Dept. of Mechnical Engineering
College Park, MD   20742
Attn: F. Morse

University of New Mexico
Technology Applications Center
Albuquerque, NM   87131
Attn: K. E. Cox

University of Pennsylvania
113 Towne Building
Philadelphia, PA   19104
Attn: National Center for Energy
        Management & Power

BASF Wyandotte Corp.
Inorganic-Electrolytic R&D
Syandotte, MI   48192
Attn: E. Y. Weissman

Englehard Industries, Inc.
Menlo Park
Edison, NJ   08817
Attn: J. G. Colin

Union Carbide
Development Laboratory Library
P.O. Box 6056
Cleveland, OH   44101

Dr. Judith H. Ambrus
WR-33, White Oak Laboratory
Naval Surface Weapons Center
Silver Springs, MD   20910

NASA-Lewis Research Center
21000 Brookpard Road
Cleveland, OH   44135
Attn: G. M. Ault, MS 3-5
       V. Hlavin, MS 3-10
       Tech. Util. Office, MS 7-3
       L. Rosenblum, MS 49-5
       C. E. May, MS 106-1
       J. S. Fordyce, MS 302-1
       D. G. Soltis, MS 309-1
       N. T. Musial, MS 500-113
       J. E. Bolander, MS 500-312
       Library, MS 60-3
       Report Control, MS 5-5

National Aeronautics & Space Admin.
Washington, D.C.   20546
Attn: L. Holcomb, Code RP-6
       S. V. Manson, Code NT
       P. R. Miller, Code NE
       R. LaRock, Code NE
       Tech. Util. Office, Code KT

NASA-Goddard Space Flight Center
Greenbelt, MD   20771
Attn: F. Ford (Code 711.2)
       G. Halpert (Code 711.2)

NASA-Langley Research Center
Instrument Research Division
Hampton, VA   23365
Attn: J. E. Zanks, MS 488

NASA-George C. Marshall Space
  Flight Center
Huntsville, AL   35812
Attn: C. B. Graff, Code EO-11

NASA-Johnson Space Center
Houston, TX   77058
Attn: J. B. Trout, EP-5

NASA-Ames Research Center
Moffett Field, CA   94035
Attn: J. Ribenzer, MS 24408

Jet Propulsion Laboratory
4800 Oak Grove Drive
Pasadena, CA   91103
Attn: A. A. Uchiyama, MS 198-22

Douglas Barron
Dept. 120
Delco-Remy Division GMC
2401 Columbus Avenue
Anderson, IN   46014

Commanding Officer
US Army Mobility Equip. R&D Center
Ft. Belvoir, VA   22060
Attn: Energy Conv. Research Div.
       (Code SMEFB-EE)

Commanding Officer
Picatinny Arsenal
Code SMUPA-FR-S-P
Dover, NJ   07801
Attn: M. R. Merriman

Office of Naval Research
Arlington, VA   22217
Attn: Director Power Program
       (Code 473)

Naval Ship R&D Center
Annapolis, MD   21402
Attn: J. H. Harrison
       (Code 2724)

Commanding Officer
US Naval Ammunition Depot
Crane, IN   47522
Attn: D. G. Miley
       (Code QEWE)

US Naval Observatory
4301 Suitland Road
Suitland, MD   20390
Attn: H. E. Ruskie
       (NISC-4321)

NAVAL Ordnance Laboratory
Silver Springs, MD   20910
Attn: P. D. Cole
       (Code 232)

Aero Propulsion Laboratory
Wright-Patterson AFB, OH 45433
Attn: J. E. Cooper, APIP-1

USAF Cambridge Research Laboratory
L. G. Hanscom Field
Bedford, MA 01731
Attn: E. Raskin (Wing F) CREC

Rome Air Development Center, EDS
Griffiss AFB, NY 13440
Attn: F. J. Mollura (TUGS)

National Science Foundation
RANN
Washington, D.C. 20550
Attn: L. Topper

Aeronutronic Div. of Philco Corp.
Technical Information Service
Ford Road
Newport Beach, CA 92663

Advanced Battery Support Unit
Building 429
AERE Harwell, Didcot, Berks
OX 11 ORA, England
Attn: Mr. K. T. Taylor

Aerospace Corp.
P.O. Box 95085
Los Angeles, CA 90045
Attn: Library Acquisition Group

American University
Chemistry Department
Mass. & Nebraska Aves., NW
Washington, D.C. 20016
Attn: R. T. Foley

Argonne National Laboratory
Chemical Engineering Division
9700 South Cass Avenue
Argonne, Illinois 60439
Attn: P. Nelson

Arthur D. Little, Inc.
Acorn Park
Cambridge, MA 02140
Attn: J. Parry

Atomics International Division
International Corp.
P.O. Box 309
Canoga Park, CA 91304
Attn: H. L. Recht

Battelle Memorial Institute
Electrochem. Eng. Tech. Div.
505 King Avenue
Columbus, OH 43201
Attn: J. E. Clifford

Bell Laboratories
Murray Hill, NJ 07974
Attn: D. O. Feder

Borden Chemical Co.
Central Research Laboratory
P.O. Box 9524
Philadelphia, PA 19124

Burgess Battery Co.
Chief Eng., Foot of Exchange
Freeport, IL 61032
Attn: M. E. Wilke

Argonne National Laboratory
Chemical Engineering Division
9700 South Cass Avenue
Argonne, IL 60439
Attn: Technical Library

Dr. James Birk
EPRI
3412 Hillview Avenue
P.O. Box 10412
Palo Alto, CA 93404

Dr. Mark Salomon
Power Sources Technical Area
Electronics Technology &
  Devices Laboratory
US Army Electronics Command
Fort Monmouth, NJ 07703
Attn: DRSEL-TL-PR